INORGANIC CHEMISTRY FRONTIERS

RESEARCH ARTICLE

View Article Online
View Journal | View Issue

Check for updates

Cite this: *Inorg. Chem. Front.*, 2025, **12**, 6257

Heteronuclear Eu_2Pt_2 luminescent arrays: composition–thermometric properties correlations†

Marco Bazi,[a] Matteo Tomassoni,[a] Luca Bellucci,[a] Gregorio Bottaro,*[b] Marzio Rancan,[b] Simona Samaritani,[a] Lidia Armelao[c,d] and Luca Labella*[a]

Lanthanide dinuclear complexes $[Ln_2(tta)_6(\mu\text{-pyrzMO})_2]$ (Ln^{3+} = Eu^{3+} and Gd^{3+}; Htta = thenoyltrifluoroacetone; pyrzMO = pyrazine-*N* oxide) can behave as ligands for the synthesis of molecular heterometallic complexes. Fast reactions at room temperature occur with $[Pt(\mu\text{-Cl})Cl(EPh_3)]_2$ (E = P, As) affording as a single product $[Ln_2(tta)_6(\mu\text{-pyrzMOPtCl}_2EPh_3)_2]$ (E = P, Ln = Eu, **1**; Ln = Gd, **2**); (E = As, Ln = Eu, **3**; Ln = Gd, **4**). Similarly, the new platinum compound [PtClppy(pyrzMO)], **5**, obtained reacting $[Pt(\mu\text{-Cl})ppy]_2$ (ppy = 2-phenylpyridine) with pyrzMO and structurally characterized through XRD, has been used to prepare $[Ln_2(tta)_6(\mu\text{-pyrzMOPtClppy})_2]$ (Ln = Eu, **6**; Ln = Gd, **7**) starting from the anhydrous formally unsaturated $[Ln(tta)_3]$ fragments. XRD studies on all heterometallic compounds have established a tetranuclear Ln_2Pt_2 molecular structure with the platinum fragment coordinated to the nitrogen atom of the pyrazine while the *N*-oxide donor functionality is bridging two lanthanide centres as in the dinuclear lanthanide precursors. PL and thermometric properties of the Eu^{3+} complexes are strongly correlated with the nature of the ligand coordinated to Pt that is PPh_3, $AsPh_3$ and ppy. Upon UV excitation, **1** and **3** exhibit intense red emission, typical of Eu^{3+} ions, with a luminance of ~10 cd m^{-2} significantly higher than that of **6** (~0.3 cd m^{-2}). Temperature-induced variations in emission intensity have been exploited to develop a series of luminescent thermometers. The integrated intensity of the $^5D_0 \rightarrow {}^7F_2$ europium transition can be used as the thermometric parameter (Δ). **1** and **3** reach S_r = 1 at around 200 K, while **6** exhibits a steeper decay in Δ, achieving S_r = 1 at approximately 100 K. For **1** and **3**, the temperature sensitivity is related to non-radiative deactivation channels involving the platinum-containing fragment and tta ligands. For **6**, instead, the interactions are limited only to the Pt-containing fragment.

Received 3rd April 2025,
Accepted 30th May 2025

DOI: 10.1039/d5qi00893j

rsc.li/frontiers-inorganic

Published on 30 Mee 2025. Downloaded on 30.05.26 06:27:56.

Introduction

In the last two decades, the synthesis and the study of luminescent d–f heterometallic assemblies showed a growing interest in the literature.[1] A d transition metal fragment can function as an antenna[2–6] enabling an indirect excitation pathway that sensitizes luminescence. It often combines chemical and photochemical stability, tunable strong light absorption, and access to long-lived excited states capable of efficiently transferring energy mostly to near-infrared emissive lanthanides [Pr(III), Nd(III), Er(III), Yb(III)],[7–12] but also to visible emissive europium and terbium.[13–20] Incorporating diverse metal ions can enhance functional properties or even enable the introduction of entirely new functionalities. However, the preparation of these d–f arrays is frequently hampered by the complexity of lanthanide coordination chemistry and the rational synthesis of targeted d/f heterometallic architectures presents a significant challenge. A common synthetic strategy relies on the use of d-block complexes bearing a pendant donor site able to bind a formally unsaturated lanthanide fragment.[21–30] The d-block complex is behaving as a ligand in a fast reaction occurring in mild conditions. This synthetic approach, involving a d metallo-ligand can normally guarantee a control of the reaction outcome, both yielding extended structure compounds or well-defined molecular architectures. The use of f metallo-ligands in the synthesis of d/f complexes has been reported in a limited number of examples, and it is normally associated with lanthanide complexes coordinated by polyden-

[a]*Dipartimento di Chimica e Chimica Industriale and CIRCC, Università di Pisa, via Giuseppe Moruzzi 13, I-56124, Italy. E-mail: luca.labella@unipi.it*
[b]*CNR ICMATE and INSTM, presso Dipartimento di Scienze Chimiche, Università di Padova, via Marzolo 1, I-35131, Italy. E-mail: gregorio.bottaro@cnr.it*
[c]*Dipartimento di Scienze Chimiche and INSTM, Università di Padova, via Marzolo 1, I-35131, Italy*
[d]*Dipartimento di Scienze Chimiche e Tecnologie dei Materiali (DSCTM) Consiglio Nazionale delle Ricerche, Piazzale A. Moro 7, 00185 Roma, Italy*

†Electronic supplementary information (ESI) available: Additional spectroscopic and crystallographic data. CCDC 2395042–2395045 and 2395089. For ESI and crystallographic data in CIF or other electronic format see DOI: https://doi.org/10.1039/d5qi00893j

Published on 30 Mee 2025. Downloaded on 30.05.26 06:27:56.

tate ligands bearing pendant functional groups.[31–36] The synthesis of mononuclear lanthanide metallo-ligands [Ln(dike)$_3$pyterpy] (Htta = 2-thenoyltrifluoroacetone and Ln = La, Y, Eu; Hhfac hexafluoroacetylacetone, and Ln = Eu, Yb) able to behave as nucleophiles in the bridge splitting reaction of the dinuclear platinum complex [Pt(μ-Cl)Cl(PPh$_3$)]$_2$ yielding heterometallic rare-earth platinum complexes, [Ln(dike)$_3$pyterpyPtCl$_2$PPh$_3$] has been recently reported.[37] Examples of molecular heterometallic platinum lanthanide complexes have been reported in the literature using platinum polypyridyl-functionalized acetylides precursors, able to bind lanthanide centres.[38–43] Interest in molecular heterometallic europium/platinum compounds is continuously growing due to their potential biomedical applications.[44–49]

A family of luminescent Eu^{3+} dinuclear complexes with general formula [Eu$_2$(β-dike)$_6$(*N*-oxide)$_y$] (Hβ-dike = Htta; dibenzoylmethane, Hdbm; benzoyltrifluoroacetone, Hbta; *N*-oxide = pyrazine-*N*-oxide, pyrzMO; 4,4′-bipyridine-*N*-oxide, bipyMO); (y = 2); (Hβ-dike = Hhfac; *N*-oxide = pyrzMO; bipyMO); (y = 3) has been recently prepared to study the effect of the β-diketonato and *N*-oxide ligands on their thermometric properties.[50,51] The products were obtained in mild conditions and in high yields reacting stoichiometric amounts of anhydrous lanthanide β-diketonates and the heterotopic ligands in toluene. X-ray single crystal studies revealed that, in all compounds, the heterotopic ligands exhibit hypodentate coordination, bridging the two lanthanide centres exclusively through the oxygen atom while featuring a pendant nitrogen atom.[51] The luminescence and thermometric properties have been found to be dependent both from the diketonate and the *N*-oxide so that they can be modulated using different building blocks. An alternative approach to controlling emission properties could involve coordinating a second metal center—platinum, in our choice—to the nitrogen atom of the hypodentate ligand, utilizing the dinuclear lanthanide precursors as metallo-ligands. Notably, a recent paper reports that heterometallic Ln$_4$Pt$_6$ molecular aggregates (Ln = Eu, Yb) exhibit temperature-dependent emission.[52] However, to the best of our knowledge, no studies in the literature have explored the modulation of thermometric properties through the incorporation of different platinum fragments into a molecular heterometallic d/f architecture. In this work, we report that the simple dinuclear complexes [Ln$_2$(tta)$_6$(*N*-oxide)$_2$], (Ln = Gd, Eu) can be used as metallo-ligands for the synthesis of heterometallic tetranuclear lanthanide platinum complexes [Ln$_2$(tta)$_6$(μ-pyrzMOPtCl$_2$EPh$_3$)$_2$] (Ln = Eu, E = P, **1**, E = As, **3**; Ln = Gd, E = P, **2**, E = As, **4**) involving the coordination of a platinum fragment to each pendant nitrogen donor, Scheme 1a. The same tetranuclear array [Ln$_2$(tta)$_6$(μ-pyrzMOPtClppy)$_2$] (Ln = Eu, **6**; Gd, **7**, Hppy: 2-phenylpyridine) can be obtained from a pyrzMO-coordinated platinum precursor, Scheme 1b.

In these compounds, the photophysical and temperature-dependent emission properties are modulated by the introduction of different platinum fragments. In fact, upon illumination with ultraviolet light, europium complex powders emit characteristic red light due to Eu^{3+} ions. The luminescence of **1** and **3**, visible to the naked eye, is more intense than that of **6**, highlighting the crucial role of platinum-containing fragments in determining emission properties. A similar behaviour is observed when the luminescence of these complexes is studied as a function of temperature between 80 and 300 K.

Results and discussion

Synthesis and X-ray structural studies

Dinuclear well-characterized β-diketonato complexes [Ln$_2$(tta)$_6$(μ-pyrzMO)$_2$], (Ln = Eu, Gd)[51] have been used here as air stable, convenient precursors for the synthesis of molecular heterometallic complexes. The major point is the availability of a pendant nitrogen donor site able to interact with a different metal centre so that the lanthanide complex can behave as a ligand. A dichloromethane solution of the dinuclear lanthanide precursor reacts at room temperature in few minutes with dinuclear chloride bridged platinum complexes [PtCl(μ-Cl)EPh$_3$]$_2$ (E = P[53–55] and As[56]) with a well-known, reactivity towards nucleophiles. A ring-opening reaction affords the kinetic *trans* products,[57–62] directed by the *trans* effect exerted

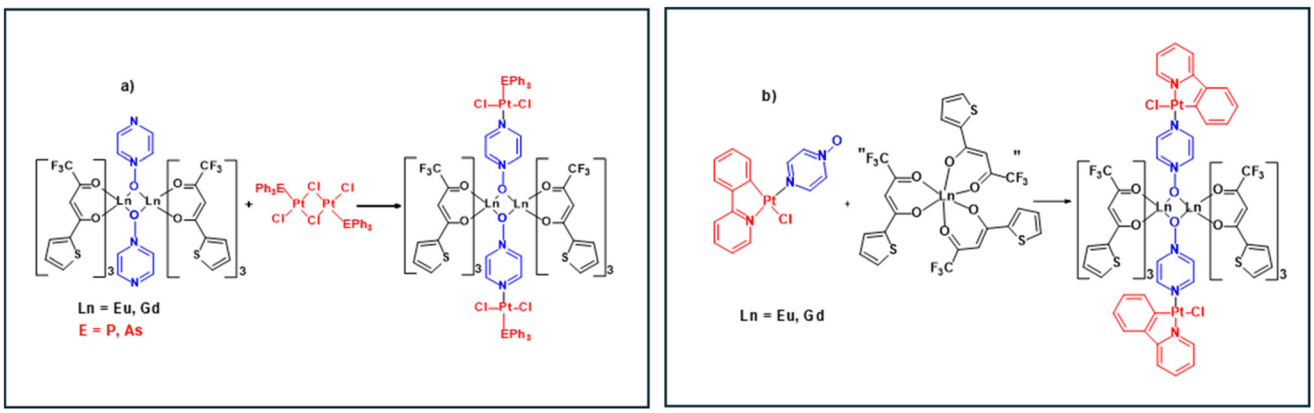

Scheme 1 Access to d/f heteronuclear Ln$_2$Pt$_2$ arrays. In (b) quotation marks indicate an unsaturated fragment containing Ln.

 This journal is © the Partner Organisations 2025

Published on 30 Mee 2025. Downloaded on 30.05.26 06:27:56.

by the triphenylphosphino or triphenylarsino ligand. The platinum precursor, initially sparingly soluble in dichloromethane, dissolves upon the formation of the heterometallic Ln/Pt product, resulting in a yellow solution within a few minutes. No side product is present if a rigorous control of the stoichiometry of reaction is observed. The product can be precipitated by the addition of heptane, obtaining in each case a bright yellow powder. Analytical data support the formation of the expected heterometallic complexes with formula $[Ln_2(tta)_6(\mu\text{-pyrzMOPtCl}_2EPh_3)_2]$ (Ln = Eu, E = P, **1**, E = As, **3**; Ln = Gd, E = P, **2**, E = As, **4**). IR spectra resemble those of the lanthanide precursor, suggesting that the dinuclear lanthanide core is maintained in the reaction with the platinum species (Fig. S1 and S2†). Pentane vapours diffusion into a chloroform or dichloromethane solution of the products yield single crystals of **1**, its Gd analogue **2**, and **3** suitable for X-ray diffraction studies (Fig. 1a–c and Table S1†). Compound **1** crystallizes in the $P2_1/n$ space group (SG), compound **2** in the $C2/c$ SG, and compound **3** in the $P\bar{1}$ SG. In each case, the structures feature an inversion centre located at the midpoint of the Ln_2O_2 core, stabilized by two bridging pyrzMO ligands. The crystal packing results in a network of voids that accommodate solvated chloroform molecules that are lost upon drying. In the molecular structures of the heterometallic compounds, the $[Ln_2(tta)_6(pyrzMO)_2]$ dinuclear core of the precursor is preserved, with pyrzMO bridging the two lanthanide centres solely through its oxygen atom (μ-O), while its nitrogen site is coordinated to platinum. Thus, the heterotopic divergent ligand effectively bridges the lanthanide and platinum centers by exploiting their differing affinities for oxygen and nitrogen donors. The Ln···Ln and Pt···Pt distances are 4.2101(7) Å and 14.9870(7) Å for **1**, 4.2617(12) Å and 14.7089(8) Å for **2**, 4.2999(8) Å and 14.8335(9) Å for **3**.

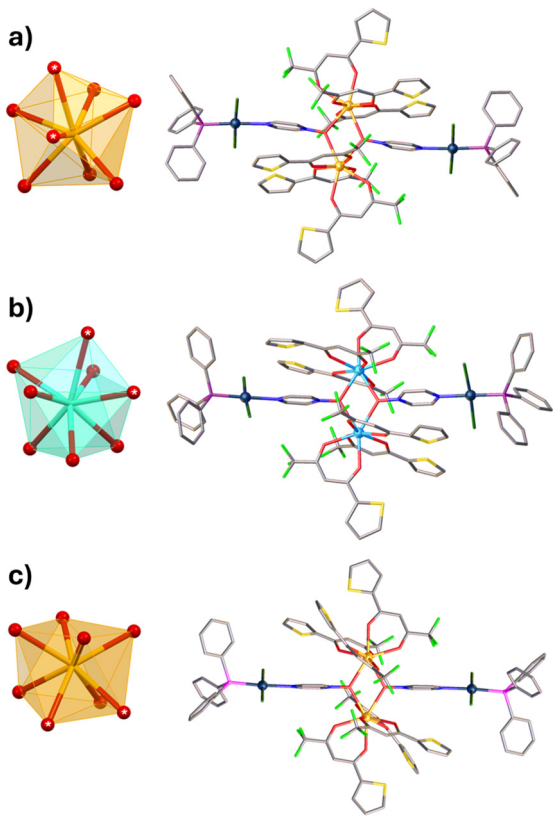

Fig. 1 Molecular structure and coordination polyhedra of the LnO_8 core for (a) **1**, (b) **2**, (c) **3** Solvent molecules, hydrogen atoms and disordered parts are omitted for clarity. Colour code: C, grey; O, red; N, blue; S, yellow; F, light green; Cl, dark green; P, violet; As, pink; Pt, dark blue; Eu, orange; Gd, azure. Oxygen atoms marked with the white asterisk belong to the bridging pyrzMO units.

In these compounds, the Ln centres show a coordination number of 8 due to the three chelating β-diketonates and the two bridging pyrzMO units. A stereochemical study of the eight-vertex polyhedra was performed by means of continuous shape measures (CShM). Calculations (SHAPE 2.1)[63] of the degree of distortion of the LnO_8 core with respect to an ideal eight-vertex polyhedron show that the coordination geometry is closer to a triangular dodecahedron for **1** and **3**, and to a square antiprism for **2** (Table S3†). A square planar geometry of the *trans* isomer is observed for platinum as expected. Compound **4** is isostructural with its europium analogue (Tables S1† and **S2**).

Experimental evidence confirms the incorporation of a platinum fragment at room temperature appended to an almost unchanged dinuclear lanthanide core. Remarkably, the lanthanide precursor $[Ln_2(tta)_6(\mu\text{-pyrzMO})_2]$ behaves here as a f-based metallo-ligand.

The dinuclear core with *O*-bridging *N*-oxide fragments has frequently been observed in previous studies with tris-diketonato lanthanide fragments,[64–68] demonstrating its high stability. In principle, a platinum precursor with a *N*-coordinated hypodentate pyrzMO ligand is expected to behave as free pyrzMO in the coordination to the formally unsaturated lanthanide fragment thereby stabilizing a dinuclear lanthanide unit.[51] For this reason, a different synthetic approach was envisaged when the sparingly soluble dinuclear $[Pt(\mu\text{-Cl})(ppy)]_2$,[69–71] (ppy = orthometalated phenylpyridine) was considered. As a matter of fact $[Pt(\mu\text{-Cl})(ppy)]_2$ was normally obtained as a greenish and not easy to purify solid and was not reasoned to be a suitable precursor for a reaction with a lanthanide metallo-ligand to be carried out with rigorous stoichiometric molar ratios of the reactants. A procedure starting from a formally unsaturated lanthanide fragment and a platinum metallo-ligand with a *N*-coordinated hypodentate pyrzMO can afford the same molecular architecture for heterometallic Ln_2Pt_2 complexes.

The platinum complex [PtCl(ppy)pyrzMO] (**5**) is synthesized by reaction of the dinuclear $[Pt(\mu\text{-Cl})(ppy)]_2$ with two equivalents of pyrzMO in THF, in a straightforward reaction. The soluble product is separated by traces of a dark solid and precipitated from a bright yellow solution with heptane. Analytical and spectroscopic data agree with the expected composition, showing through NMR the presence of a single species in solution (Fig. S4 and S5†), the *SP*4-4 isomer, identified through SC-XRD. The molecular structure (Fig. 2) shows the pyrzMO

Published on 30 Mee 2025. Downloaded on 30.05.26 06:27:56.

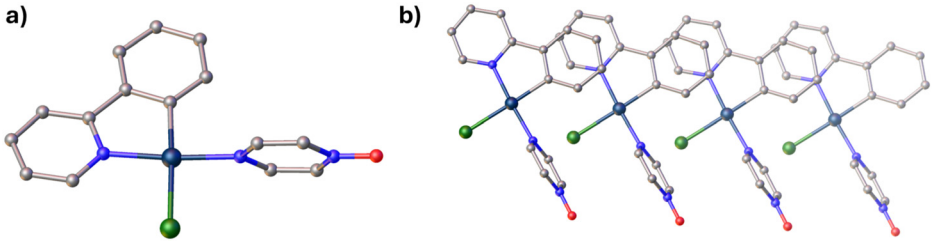

Fig. 2 (a) Molecular structure of **5** and (b) staggered stacking. Colour code: C, grey; O, red; N, blue; Cl, dark green; Pt, dark blue.

ligand bonded to platinum only through the nitrogen atom. The oxygen donor site is not involved in any significant bonding interaction. In the crystal structure, complex **5** assembles into one-dimensional supramolecular chains through staggered stacking interactions between the phenylpyridine rings, with an average inter-ring distance of 3.5 Å (Fig. 2b).

In agreement with our data, several literature reports present a bridge-cleavage reaction of the dinuclear [Pt(μ-Cl)(ppy)]$_2$ complex for a pyridine-based ligand yielding an initial mononuclear *SP*4-3 isomer, due to the strong *trans* effect exerted by the aryl donor, and to the successive isomerization to the thermodynamically more stable *SP*4-4 isomer form.[72–74]

5 promptly reacts with one equivalent of [Ln(tta)$_3$] (Ln = Eu, Gd) in dichloromethane at room temperature with an initial bright yellow solution turning into a bright red solution. The reaction product, yellow-orange in colour, is precipitated by adding heptane and presents analytical data supporting the stoichiometry 1 to 1 of the two metal fragments. The IR spectra showed several similarities with the dinuclear complex [Ln$_2$(tta)$_6$(μ-pyrzMO)$_2$] suggesting the formation of a dinuclear lanthanide core (Fig. S3†). The molecular structure of the tetranuclear Pt_2Eu_2 complex **6** was elucidated through SC-XRD showing the presence of the dinuclear lanthanide core in which the oxygen atoms of two pyrzMO bridge two europium centres similarly to the molecular precursor [Eu$_2$(tta)$_6$(μ-pyrzMO)$_2$] (Fig. 3). Compound **6** crystallizes in the $P2_1/n$ space group. The Eu···Eu and Pt···Pt distances are 4.270(4) Å and 14.648(3) Å, respectively. As found in the above discussed structure, an inversion centre is located at the midpoint of the Eu_2O_2 core. A stereochemical study of the eight-vertex polyhedron by means of CShM shows that the minimal degree of distortion of the EuO_8 core with respect to an ideal eight-vertex polyhedron is reached for the square antiprism geometry (Table S3†). The nitrogen donor atom of the heterotopic divergent ligand is bonded to platinum in a *SP*4-4 isomer. The molecular structure of **6** closely resembles that of **1** and **2** despite the different synthetic approach. [Gd$_2$(tta)$_6$(μ-pyrzMOPtClppy)$_2$], **7**, has been found to be isostructural with **6** (Tables S1 and S2†). **5** uses the oxygen donor functionality to bind two lanthanide unsaturated fragments in fast reactions and mild conditions, behaving as the free pyrzMO moiety.

These results show that the dinuclear lanthanide unit [Ln$_2$(tta)$_6$(μ-pyrzMO)$_2$] is sufficiently inert to be used as a f-based metallo-ligand and that this dinuclear core is sufficiently stable to be formed in mild conditions also starting from the platinum precursor **5** and [Ln(tta)$_3$] (Ln = Eu, Gd).

Room temperature photoluminescence. Recently, we have focused our attention on di- or tetra- nuclear complexes consisting of [Ln(β-dike)$_3$] units connected through *N*-oxide ligands.[51,67,68] We observed that the room temperature emission properties and the temperature sensing characteristics in this class of compounds are strongly correlated with the struc-

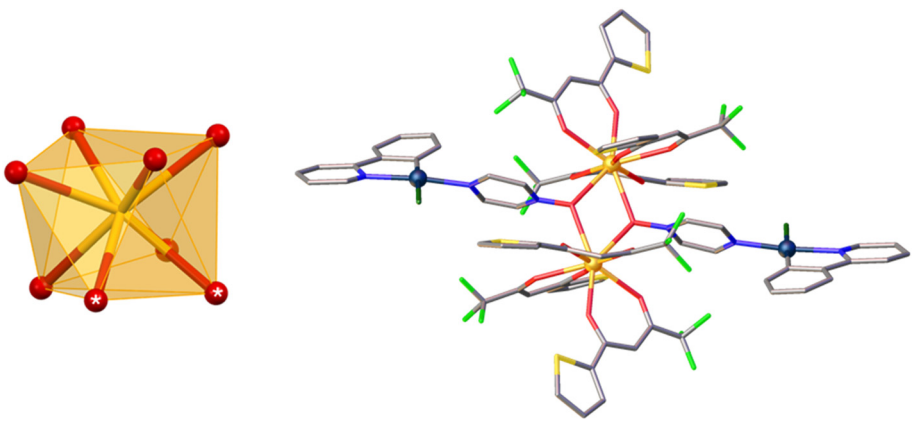

Fig. 3 Molecular Structure and coordination polyhedron of the EuO_8 core for **6**. Hydrogen atoms and disordered parts are omitted for clarity. Colour code: C, grey; O, red; N, blue; S, yellow; F, light green; Cl, dark green; Pt, dark blue; Eu, orange. Oxygen atoms marked with the white asterisk belong to the bridging pyrzMO units.

 This journal is © the Partner Organisations 2025

Published on 30 Mee 2025. Downloaded on 30.05.26 06:27:56.

ture of the ligands. Ligand-centred electronic transitions and charge transfer between metal and ligand play a crucial role in defining the spectroscopic and functional characteristics of the complexes.[51,67,68,75–77] In this study, we exploit *N*-oxide ligands to synthesize heterometallic d–f complexes, achieved by coupling $[Ln(tta)_3]$ with platinum-based fragments. This approach aims to explore the ability of Pt moieties to modulate the emission properties of Ln^{3+} centres.

Pt(II) complexes have been extensively studied due to their distinctive photophysical behaviour as triplet emitters. Their absorption and emission characteristics can be finely tuned by modifying the electronic and steric properties of the coordinating ligands. In particular, bulky ancillary ligands are often employed to suppress Pt···Pt interactions, which are favoured by the nearly square-planar geometry of Pt(II) centres. These interactions can promote aggregate formation, leading to red-shifted emissions and reduced colour purity. Additionally, ligands containing heavy atoms are frequently introduced to enhance spin–orbit coupling, thereby facilitating intersystem crossing and improving triplet emission efficiency.[78–81]

The range of available Pt(II) complexes with well-characterized electronic properties is vast. Therefore, selecting an appropriate Pt complex for the synthesis of heterobimetallic Eu_2Pt_2 complexes is nontrivial. In this study, we focused on two structural classes: (i) complexes featuring pnictogen-based neutral donors (*e.g.*, $PtCl_2(PPh_3)$ and $PtCl_2(AsPh_3)$), and (ii) cyclometalated Pt(II) complexes, specifically PtCl(ppy), where ppy = 2-phenylpyridine. The latter represent one of the most thoroughly investigated families of Pt(II) emitters, with ppy often considered the prototypical cyclometalating ligand. In contrast, ligands such as triphenylarsine ($AsPh_3$) have been much less explored compared to their phosphorus analogue (PPh_3). Nonetheless, we found them intriguing because in Pt(II) complexes of the general formula $PtL(PnPh_3)$ (Pn = P, As, Sb), a systematic red shift in the energy of electronic transitions is observed along the pnictogen series from P to Sb, and a hyperchromic shift (increase in the intensity of a spectral band) can be observed as well.[80–83] The bathochromic shift, typically on the order of several hundred cm^{-1}, can significantly influence the luminescence behaviour of Eu_2Pt_2 systems, particularly when the relevant excited-state energies fall within 17 000–18 000 cm^{-1}, *i.e.*, near the $^5D_0$ emitting level of Eu^{3+}.

The study of the absorption spectra of the Gd_2Pt_2 and Eu_2Pt_2 complexes provides information on the nature of the electron transitions in this family of complexes.

Simply looking at the sample powders we can divide them into two groups based on their colours. In fact, **1** and **3** appear as bright yellow powders while **6** is darker with orange tones.

To evaluate the effect of Pt-based fragments, it is useful to first identify the spectral features associated with the $[Ln_2(tta)_6(\mu\text{-pyrzMO})_2]$ core. The solid-state absorption spectrum of $[Gd_2(tta)_6(\mu\text{-pyrzMO})_2]$ (Fig. S6†) displays a broad band primarily located in the UV region, with an absorption onset around 420 nm. In contrast, the spectrum of $[Eu_2(tta)_6(\mu\text{-pyrzMO})_2]$ exhibits a markedly different profile, characterized by a sharp peak at 415 nm and a pronounced tail extending across most of the visible range. This feature is attributed to ligand-to-metal charge transfer (LMCT) transitions.[84–91]

The diffuse reflectance spectra of the Ln_2Pt_2 complexes (Fig. 4 and Fig. S7†) are significantly broadened and extend further into the visible region. The absorption onsets are observed around 500 nm for complexes **1** and **2**, 530 nm for complexes **3** and **4**, and approximately 600 nm for complexes **6** and **7**.

In general, Pt(II) complexes exhibit intense absorptions in the UV region (*ca.* 260–330 nm), attributed to ligand-centred $\pi \rightarrow \pi^*$ and $n \rightarrow \pi^*$ transitions, along with broad LMCT bands that extend into the visible region.[41,78–83] Accordingly, the absorption spectra of Gd_2Pt_2 (Fig. 4a) and Eu_2Pt_2 (Fig. 4b)

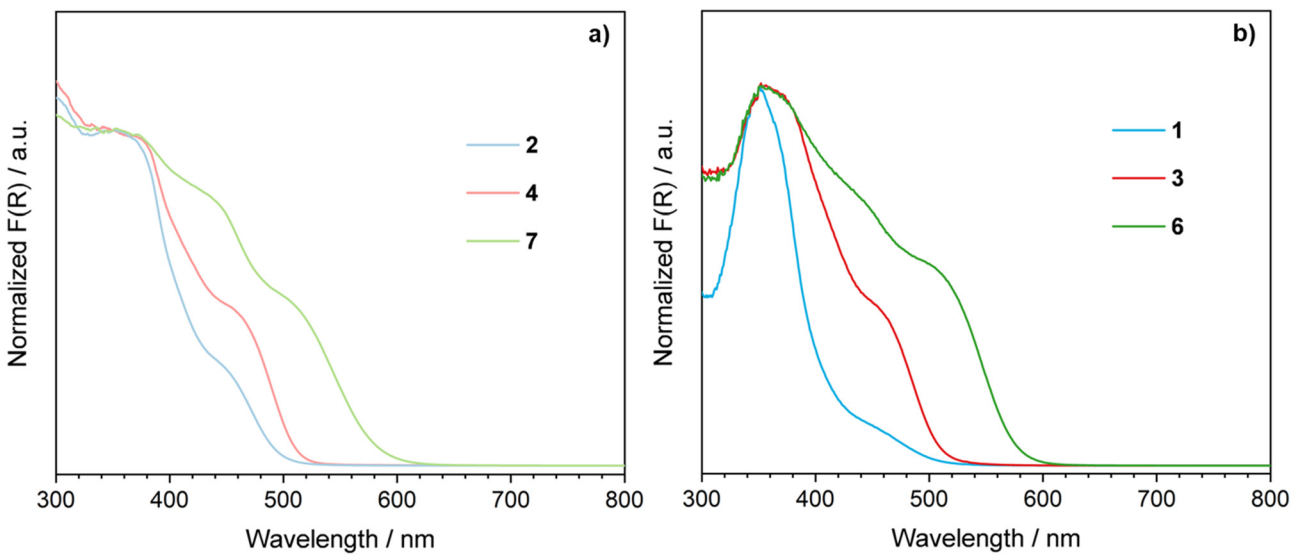

Fig. 4 Diffuse reflectance absorption spectra of the powders of (a) Gd_2Pt_2 and (b) Eu_2Pt_2 complexes.

Published on 30 Mee 2025. Downloaded on 30.05.26 06:27:56.

complexes can be conceptually divided into two regions: below 400 nm, where ligand-centred transitions dominate, and above 400 nm, where the absorptions are primarily associated with MLCT transitions.

For the gadolinium series, the visible-region absorptions are exclusively attributed to MLCT transitions involving the Pt(II) moieties. The absorbed portion of visible light varies with the nature of the Pt(II) fragment, following the trend: $PtCl_2(PPh_3)$ < $PtCl_2(AsPh_3)$ < PtCl(ppy). In the Eu_2Pt_2 complexes, the overall band assignment parallels that of the Gd analogues. However, the high-energy portion of the MLCT envelope results from a combination of transitions involving both Pt and Eu centres (Fig. S6 and S7†).

Therefore, similarly to what observed in other heterobimetallic complexes,[84] Eu^{3+} emission can be sensitized through two excitation paths involving the two kinds of ligands. In general, ligand-centred energy levels close to Eu^{3+} excited states favour non-radiative deactivation mechanisms. While these mechanisms may reduce the brightness of the emitters, they can positively influence their thermometric properties.[92]

The excitation spectra (PLE) of **1** and **3** (Fig. 5a) show broad signals in the ultraviolet region with a tail extending up to approximately 450 nm. Below 400 nm, the PLE spectrum of **6** is similar to those of **1** and **3**. However, **6** exhibits a shoulder in the visible region that is absent in the spectra of the other two complexes, which is ascribed to transitions centred on the Pt-moiety. In fact, while the emission spectra of **1** and **3** show the typical well-resolved multiplets of europium, in the emission spectrum of **6** the signals due to the transitions from the $^5D_0$ excited state to the fundamental multiplets ^7F_J (J = 0, 1, 2, 3 and 4) of Eu^{3+} are broader and emerge from a background due to the emission, of comparable intensity, of the Pt-containing fragment (Fig. 5b and S8†). The emission of europium occurs by indirect excitation exploiting the absorption properties of the organic ligands and the energy transfer from ligand-centred triplet states to the emitting levels of the metal ion according to the well-known scheme that characterizes the "antenna process". In addition to the shape of the spectra, the different behaviour of the complexes is also visible to the naked eye. In fact, when **1** and **3** powders are illuminated with ultraviolet light a bright red luminescence is observed. In contrast, under the same illumination conditions the light emission from **6** powders is faint.

To compare the emission performance of different emitters, quantification of the emitted light in certain conditions is required. To this aim, the most frequently used parameter is the photoluminescence quantum yield (PLQY) which for solid samples should be measured using an integrating sphere. Besides problems related to the measurements that can be tricky, the major drawback of PLQY is that it provides a partial indication. PLQY gives us information "only" on the fraction of absorbed photons that are re-emitted, but it does not provide information about the number of absorbed photons nor on the capability of the sample to absorb light. Or better, these data are used to calculate PLQY but seldom explicitly reported. In other words, to have an intense emission, a molecule or a material should absorb as many photons as possible and the PLQYs should be equal to 1. In solution the ability of a molecule to absorb light is given by the molar extinction coefficient. Therefore, for luminescent molecules in solution, a good parameter to quantify the amount of emitted light is the brightness (B = PLQY × ε), *i.e.* the product between PLQY and the molar absorption coefficient. In solid state the situation is more complicated, and the determination of an absorption coefficient is not trivial. In addition, in different fields of application, brightness can have different definitions. These aspects have been critically analyzed recently.[93,94] Alternatively, to quantify the intensity of the emitted light and

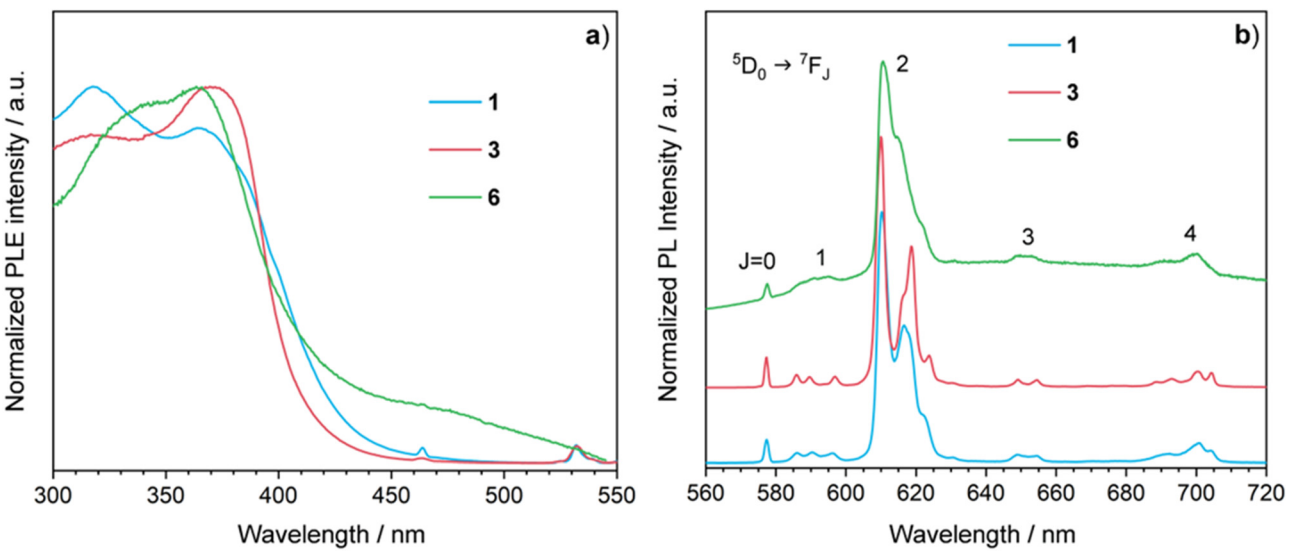

Fig. 5 (a) Photoluminescence Excitation (PLE) spectra monitored on the most intense Eu^{3+} emission peak. (b) Emission spectra of Eu^{3+}-containing complexes excited at 375 nm.

 This journal is © the Partner Organisations 2025

Published on 30 Mee 2025. Downloaded on 30.05.26 06:27:56.

Table 1 Experimental lifetimes (τ_{exp}), radiative lifetimes (τ_{rad}), photoluminescence quantum yields (PLQY), intrinsic quantum yields (Φ), and sensitization efficiencies (η) and luminance. All PL data are obtained exciting the samples at 375 nm

Sample	T^a (10^3 cm^{-1})	τ_{exp} (μs)	τ_{rad} [b] (μs)	Φ [b] %	PLQY %	η [c] (%)	Luminance[d] (cd m^{-2})
1	18.2–20	206	1114	18	2.5	14	9.3
3	18.2–20	216	1139	19	2.5	13	10.5
6	18.2–15.8	52	810	6	—	—	0.3

[a] Determined from 80 K emission spectra (Fig. S9†) of Gd-complexes (**2**, **4**, **7**).[95] Since the 0–0 vibronic band is not clearly observed the interval between the peak onset and first observed maximum is reported. [b] Value calculated following a well-established procedure.[84,95] [c] η = PLQY/Φ × 100. [d] Measured illuminating the samples with a 375 nm LED with a power of 2.4 mW.

relate it to human perception of light and colours, one can use luminance (expressed in cd m^{-2}), a photometric quantity that weights the radiation intensity based on the spectral response of the human eye.[93,94] Table 1 presents a collection of spectral parameters for the examined compounds, enabling the comparison of their spectroscopic properties.

At room temperature **1** and **3** have the same absolute quantum yield (Table 1) and the sensitization efficiencies, calculated as the ratio of quantum efficiency to PLQY, is less than 20%. The europium emission is less intense than that observed in other dinuclear complexes connected by *N*-oxides, where the nitrogen donor atom is not coordinated.[51] The different behaviour is due to the presence of platinum. Consistent with the hypothesis proposed during the discussion of the diffuse reflectance absorption spectra (Fig. 4), MLCT of platinum-containing moieties introduce low-energy levels that favour the non-radiative deactivation of europium excited states. A comparable situation, but with more pronounced Eu^{3+} emission quenching, is observed in **6** bearing ppy ligand, which exhibits extremely weak emission, rendering its PLQY unmeasurable. It is worth noticing that the absorption spectrum of **6** is wider in the visible range than that of **1** and **3** (Fig. 4). The remarkable similarity in ligands employed for **1** and **3** accounts for their identical PLQY values and luminance, approximately 10 cd m^{-2} under 375 nm LED irradiation (2.4 mW) also indicating comparable light absorption capabilities. In contrast, **6** exhibits a significantly lower luminance of 0.3 cd m^{-2}.

Thermometric properties. Before investigating the emission behaviour of the complexes in the temperature range 80–300 K, we determined the triplet state energies of the ligands. In this family of complexes, we have two possible excitation pathways involving tta and/or Pt-containing moieties that can be considered independent as we have observed in other heterobimetallic complexes.[84] The triplet energy of tta is approximately 20 400 cm^{-1}, making it an effective sensitizer for europium.[51,91] Based on the observations at room temperature, the excitation channel involving Pt fragment is likely to determine the emission properties. The 80 K spectra of the Gd-based complexes (**2**, **4**, **7**, Fig. S9†) are entirely located at energies below 20 000 cm^{-1} with the first maximum at 18 200 cm^{-1} for **2** and **4** and 15 800 cm^{-1} for **7** (Table 1). The observed bands, which do not change regardless of the excitation wavelength, are attributable to transitions centred on the Pt-containing fragments, while signals at an energy compatible with the tta triplet are not clearly distinguishable, presumably shadowed by the transitions centred on Pt. Energy levels in close proximity to Eu^{3+} $^5D_0$ will certainly play a primary role in determining the thermometric properties of this family of complexes.

As thermometric parameter (Δ) we used the integrated intensity of the $^5D_0 \rightarrow {}^7F_2$ transition. The Δ *vs.* T curves and the relative thermal sensitivity (S_r, eqn (1)) trend are reported in Fig. 6.

$$S_r = \frac{1}{\Delta}\left|\frac{\delta\Delta}{\delta T}\right| \quad (1)$$

The $\Delta(T)$ curves of **1** and **3** exhibit very similar trends, as one would expect given the great similarity of the two compounds. The value of Δ decreases gradually with increasing temperature with a pseudo-sigmoidal trend. Regarding relative thermal sensitivity, it is noted that for these two molecules the quality factor $S_r \geq 1$ (quality criterion for using these compounds as highly sensitive luminescent thermometers) is reached at 200 K. In **6**, we note a steeper decrease in the value of Δ, S_r reaches the value of 1 already at about 100 K. This characteristic means that when **6** is used as a luminescent molecular thermometer, it has a minimum operating temperature 100 degrees lower than that of **1** and **3** and a much wider operating range (temperature range with $S_r \geq 1$). Previously, we studied other compounds of the same family[51] in which the β-diketonato units are interconnected by pyrazine *N*-oxide and 4,4′-bipyridine *N*-oxide in which S_r became greater than one at significantly higher temperatures between 250 and 300 K. In that case, the thermometric properties were determined by the energy of the triplets of the β-diketonates and by the presence of LMCT transitions.

All ligand-centred and tta-to-Eu charge transfer (CT) transitions are located at high energies (above approximately 24 000 cm^{-1}), with the latter exhibiting a long tail extending into the visible region (Fig. S6†). These energy levels are too high to play a direct role in the observed thermally induced variations in emission intensity.

At lower energies, absorption bands corresponding to metal-to-ligand charge transfer (MLCT) transitions centred on the Pt(II) moieties are observed (Fig. 4 and Fig. S6, S7†). The spectral and thermometric behaviour of the complexes is strongly influenced by the nature of the ligand coordinated to

Published on 30 Mee 2025. Downloaded on 30.05.26 06:27:56.

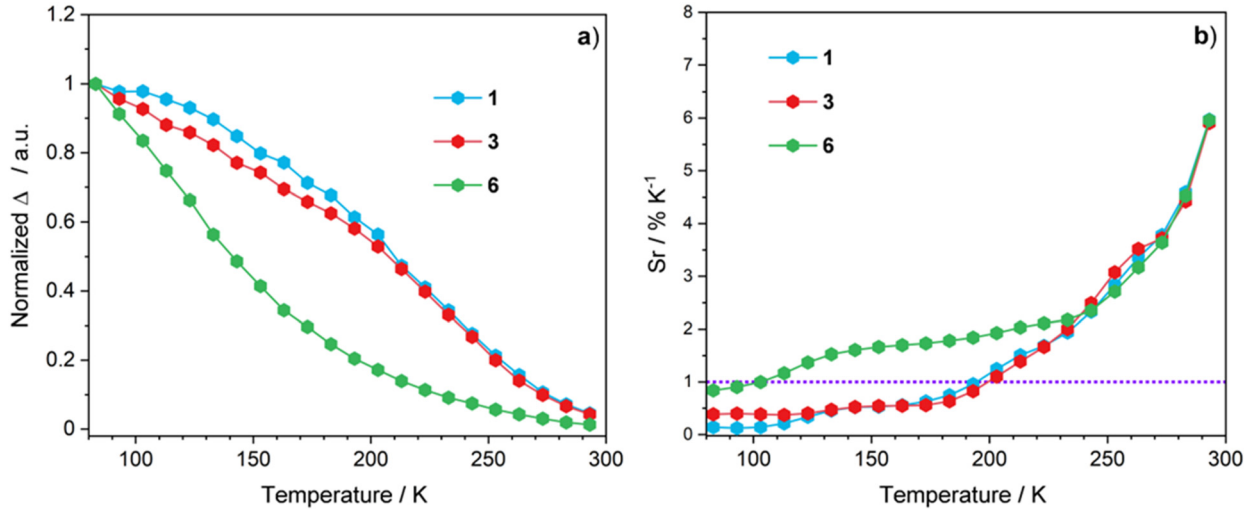

Fig. 6 (a) Thermometric parameter (Δ) and b) relative thermal sensitivity (S_r) for Eu^{3+}-containing complexes **1**, **3** and **6** (λ_{exc} = 375 nm).

Pt(II) : PPh_3 in complex **1**, $AsPh_3$ in complex **3**, and ppy in complex **6**. Triphenylphosphine and triphenylarsine ligands are electronically and sterically similar, and as a result, the spectroscopic features of complexes **1** and **3** are nearly identical (Fig. 4, 5 and Table 1). This similarity is also reflected in their thermometric performance, with $\Delta(T)$ and $S_r(T)$ curves showing matching trends. These results support the hypothesis that the thermometric behaviour of the Eu_2Pt_2 complexes is primarily governed by the photophysical properties of the Pt-based moiety.

In contrast, substituting the EPh_3 ligand with a cyclometalating ppy ligand, characterized by lower-energy MLCT states, as confirmed by both absorption and emission spectra (Fig. 4 and Fig. S7, S9†), results in markedly different thermal behaviour. Specifically, complex **6** exhibits a sharp decrease in integrated emission intensity at lower temperatures compared to complexes **1** and **3**. This leads to enhanced thermometric sensitivity in the low-temperature range.

Overall, the coordination of *N*-oxide ligands to Pt(II) to form heterobimetallic assemblies has proven to be an effective strategy to tailor the operational temperature range of luminescent thermometers.

To obtain information on the luminescence quenching mechanisms that determine the thermometric response of the complexes, we fitted the experimental Δ *vs.* T curves using the Mott–Seitz model (eqn (2)) where Δ_0 is the value of Δ at 0 K, ΔE_i the activation energy, α_i the ratio between the nonradiative and radiative deactivation probabilities for the considered path, k_B the Boltzmann constant, and T the temperature in K.

$$\Delta(T) = \frac{\Delta_0}{1 + \sum_i \alpha_i e^{-\frac{\Delta E_i}{k_B T}}} \quad (2)$$

The experimental curves of **1** and **3** can be well reproduced using a two-term model (Fig. S10†), while only one is sufficient for **6**. The activation energies are reported in Table 2.

Table 2 Mott–Seitz activation energies determined from the fitting of experimental data

Sample	ΔE_1 (cm^{-1})	ΔE_2 (cm^{-1})
1	475	2274
3	296	2187
6	357	—

Noteworthy, in all complexes there is a process with an activation energy between 300 and 500 cm^{-1} while only in **1** and **3** a second channel with a significantly higher energy (ΔE > 2000 cm^{-1}) is active. To identify the possible non-radiative deactivation pathways of the excited emitting europium states, we have constructed a simplified energy level diagram (Fig. 7).

For **1** and **3**, the two activation energies found are compatible with interactions between the excited states $^5D_0 \rightarrow {}^7F_0$ and $^5D_0 \rightarrow {}^7F_1$ of Eu^{3+} and MLCT states of –$PtPPh_3$ and –$PtAsPh_3$ moiety (Table 2, ΔE_1) and of the tta triplet (ΔE_2) indicating that both channels are active in determining the properties of these molecular thermometers. For **6**, instead, the interactions only occur with the –PtClppy fragment, as supposed in the discussion of the emission properties at room temperature.

We have also investigated the emission properties and the possible application as a molecular thermometer of **5** (Fig. 8). The absorption spectrum shows a rather broad band that extends from 500 nm down to the ultraviolet. At room temperature, exciting at the maximum of absorption, a weak emission with a lifetime of 2 μs is observed (Fig. 8b). The emission band of **5** covers almost all the visible and shows a low-energy tail that extends into the near infrared.

The observed emission band is likely due to ^{3}MLCT [Pt(5d) → π*] as commonly observed in 2-phenylpyridine cased complexes.[96] Lowering the temperature down to liquid nitro-

 This journal is © the Partner Organisations 2025

Published on 30 Mee 2025. Downloaded on 30.05.26 06:27:56.

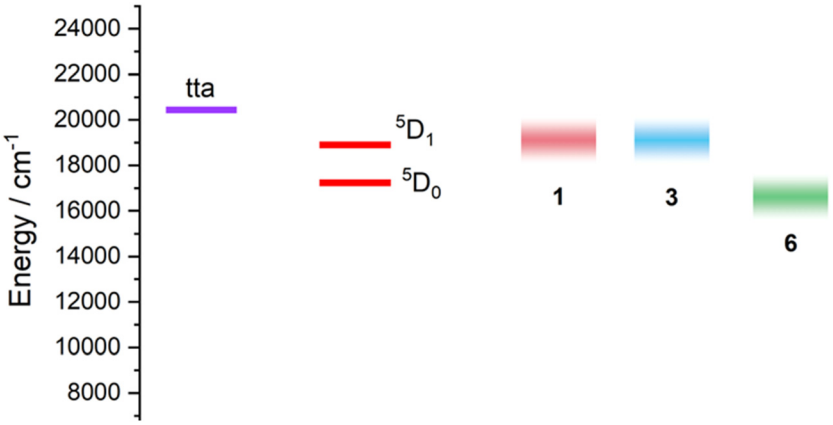

Fig. 7 Simplified energy level diagram reporting the excited states of Eu^{3+}, the triplet energy of the tta ligand, and the energy of Pt-centred MLCT states. All but tta triplet levels are indicated as boxes to evidence the uncertainties on the energy due to the lack of a vibronic progression in the spectra used for their determination (Fig. S9†). Eu^{3+}-tta MLCT are not reported due to their high energy (24 000 cm^{-1}).

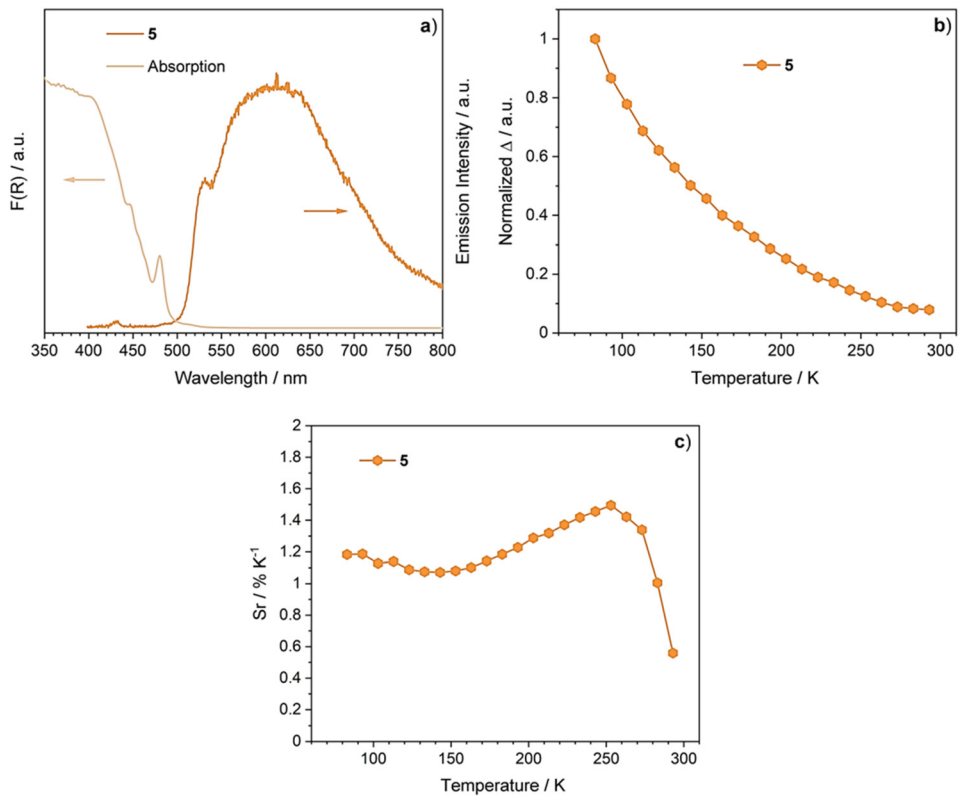

Fig. 8 Spectroscopic characterization and thermometric properties of compound **5** powders: (a) diffuse reflectance and emission spectra (λ_{exc} = 400 nm), (b) thermometric parameter Δ defined as the integrated intensity of the emission band. (c) Relative thermal sensitivity.

gen we observed an increase of the emission intensity as depicted in Fig. 8b suggesting a possible employment of this complex as molecular thermometer. S_r values are always slightly above 1% K^{-1} with small fluctuations indicating a good thermal sensitivity over a 200 K temperature range. The maximum S_r is 1.52% K^{-1} at 253 K.

Experimental section

Materials and instrumentation

All the syntheses were performed under argon atmosphere. $[Ln_2(tta)_6(\mu\text{-pyrzMO})_2]$[51] (Ln: Eu, Gd), $[PtCl(\mu\text{-Cl})EPh_3]_2$ (E: P,[53] As[56]), pyrzMO,[97] $[Pt(\mu\text{-Cl})ppy]_2$ [72] and $[Ln(tta)_3]$[98] (Ln: Eu, Gd)

Published on 30 Mee 2025. Downloaded on 30.05.26 06:27:56.

were prepared according to literature methods. All other reagents were obtained from commercial sources (Merck, Stream Chemicals, Alfa Aesar) and used as received. NMR spectra for **5** were recorded at room temperature on Jeol400 spectrometer; IR spectra were recorded in ATR (Attenuated Total Reflectance) on PerkinElmer Spectrum One or Agilent Cary630FTIR spectrometer. Elemental analysis (C, H, N) was performed at the Dipartimento di Chimica e Chimica Industriale, Università di Pisa (Italy). Absorption spectra of powder samples were recorded using a Cary 5000 UV-vis spectrometer equipped with an integrating sphere. The spectra were normalized and plotted as $F(R)$ *vs*. wavelength. $F(R)$ is the Kubelka–Munk function. Room-temperature luminescence spectra of sample powders were recorded with a Horiba JobinYvon Fluorolog-3 spectrofluorimeter. Absolute photoluminescence quantum yields (PLQYs) were calculated from corrected emission spectra obtained by means of an integrating sphere. Estimated errors on PLQY and excited-state lifetimes are ±20% and 10%, respectively. Temperature-dependence experiments (223–373 K) were carried using a Horiba T64000 triple spectrometer and a Linkam THMS600 heating/freezing microscope stage having a temperature stability of <0.1 K over an 83–873 K temperature range. Luminance measurements were performed by means of a Konica-Minolta CS-160 Luminance and Colour Meter equipped with cs135 close-up lens. Ca. 3 mg of sample powders were mixed and finely grinded with 300 mg of $BaSO_4$ and successively placed on watch glass. Luminance data, given as the average of 10 measurements, are collected normal to the sample at the minimum focusing distance of the CS-160. To excite samples luminescence a 375 nm (2.4 mW) LED powered with a bench-top stabilized power supply.

Synthesis of $[Eu_2(tta)_6(\mu\text{-pyrzMOPtCl}_2\text{PPh}_3)_2]$ (1). $[Eu_2(tta)_6(\mu\text{-pyrzMO})_2]$ (118 mg, 0.065 mmol) and $[PtCl(\mu\text{-Cl})PPh_3]_2$ (66.2 mg, 0.063 mmol) were introduced into a Schlenk flask containing 10 ml of dichloromethane. The initial orange suspension after a few minutes turned into a yellow solution. The product (**1**), precipitated by adding 50 ml of heptane was filtered off and dried *in vacuo*. Yield: 81.6% (148 mg). Anal. calcd for $[Eu_2(tta)_6(\mu\text{-pyrzMOPtCl}_2\text{PPh}_3)_2]$, $C_{92}H_{62}N_4Cl_4Eu_2F_{18}O_{14}Pt_2P_2S_6$, %: C, 38.4; H, 2.2; N, 2.0. Found: C, 38.1; H, 1.8; N, 2.0. IR-ATR (1700–1100 cm^{-1}, Fig. S1†): 1615 (s), 1596 (s), 1579 (s), 1539 (s), 1507 (m), 1468 (m), 1438 (m), 1411 (s), 1355 (m), 1311 (s), 1294 (s), 1248 (s), 1230 (s), 1188 (s), 1138 (s), 1122 (s), 1100 (m). X-Ray quality crystals were grown by slow diffusion of hexane vapour in a chloroform solution.

The Gd^{3+} derivative **$[Gd_2(tta)_6(\mu\text{-pyrzMOPtCl}_2\text{PPh}_3)_2]$** (**2**) has been obtained following a similar procedure starting from $[Gd_2(tta)_6(\mu\text{-pyrzMO})_2]$ (180 mg, 0.098 mmol), $[PtCl(\mu\text{-Cl})PPh_3]_2$ (103 mg, 0.097 mmol) in dichloromethane (10 mL). **2**: 168 mg, 59.8%. Anal. calcd for $[Gd_2(tta)_6(\mu\text{-pyrzMOPtCl}_2\text{PPh}_3)_2]$, $C_{92}H_{62}N_4Cl_4F_{18}Gd_2O_{14}Pt_2P_2S_6$, %: C, 38.2; H, 2.2; N, 1.9. Found: C, 37.9; H, 2.4; N, 1.8. IR-ATR (1700–1100 cm^{-1}, Fig. S2†): 1615 (s), 1596 (s), 1579 (s), 1539 (s), 1507 (m), 1471 (m), 1436 (m), 1410 (s), 1355 (m), 1310 (s), 1294 (s), 1248 (s), 1231 (s), 1188 (s), 1138 (s), 1122 (s), 1100 (m). X-ray quality crystals were grown by slow diffusion of pentane vapour in a chloroform solution.

Synthesis of $[Eu_2(tta)_6(\mu\text{-pyrzMOPtCl}_2\text{AsPh}_3)_2]$ (3). $[Eu_2(tta)_6(\mu\text{-pyrzMO})_2]$ (94.8 mg, 0.052 mmol) and $[PtCl(\mu\text{-Cl})AsPh_3]_2$ (59.3 mg, 0.052 mmol) were introduced into a Schlenk flask containing 10 ml of dichloromethane. The initial orange suspension after a few minutes turned into a yellow solution. The product (**3**) was precipitated by adding 50 ml of heptane in the solution, then filtered off and dried *in vacuo*. Yield: 70.7% (109.1 mg). Anal. calcd for $[Eu_2(tta)_6(\mu\text{-pyrzMOPtCl}_2\text{AsPh}_3)_2]$, $C_{92}H_{62}N_4As_2Cl_4Eu_2F_{18}O_{14}Pt_2S_6$, %: C, 37.2; H, 2.1; N, 1.9. Found: C, 36.9; H, 1.9; N, 1.8. IR-ATR (1700–1100 cm^{-1}, Fig. S1†): 1613 (s), 1595 (s), 1576 (s), 1538 (s), 1506 (m), 1467 (m), 1437 (m), 1408 (s), 1355 (m), 1311 (s), 1294 (s), 1246 (s), 1229 (s), 1188 (s), 1137 (s), 1121 (s). X-ray quality crystals were grown by slow diffusion of pentane vapour in a dichloromethane solution.

The Gd^{3+} derivative **$[Gd_2(tta)_6(\mu\text{-PyrzMOPtCl}_2\text{AsPh}_3)_2]$** (**4**) has been obtained following a similar procedure starting from $[Gd_2(tta)_6(\mu\text{-pyrzMO})_2]$ (366 mg, 0.200 mmol), $[PtCl(\mu\text{-Cl})AsPh_3]_2$ (229 mg, 0.200 mmol). **4**: 447 mg, 75.0%. Anal. calcd for $[Gd_2(tta)_6(\mu\text{-pyrzMOPtCl}_2\text{AsPh}_3)_2]$, $C_{92}H_{62}N_4As_2Cl_4F_{18}Gd_2O_{14}Pt_2S_6$, %: C, 37.1; H, 2.1; N, 1.9. Found: C, 36.9; H, 2.2; N, 1.7. IR-ATR (1700–1100 cm^{-1}, Fig. S2†): 1613 (s), 1594 (s), 1576 (s), 1538 (s), 1506 (m), 1467 (m), 1437 (m), 1408 (s), 1355 (m), 1307 (s), 1294 (s), 1247 (s), 1229 (s), 1186 (s), 1137 (s). Single crystals were grown by slow diffusion of pentane vapour in a dichloromethane solution. Although unsuitable for an X-ray study meeting publication standard, the crystals exhibited the same metric of **3**. Unit cell parameters have been reported in Table S2.†

Synthesis of [PtClppy(pyrzMO)] (5). A suspension of $[Pt(\mu\text{-Cl})ppy]_2$ (156.7 mg, 0.204 mmol) in THF (100 ml) was treated with pyrzMO (38.4 mg, 0.400 mmol) and stirred until the liquid phase of the dark-black suspension turned into a bright yellow solution. The suspension was filtered off from the dark solid residue and concentrated to half volume. A yellow solid precipitated by adding 50 ml of heptane. The product was filtered off and dried *in vacuo*. Yield: 74.1% (142.6 mg). Anal. calcd for [PtClppy(pyrzMO)], $PtC_{15}H_{12}N_3ClO$, %: C, 37.5; H, 2.5; N, 8.7. Found: C, 37.1; H, 2.4; N, 8.3. ^{1}H NMR (400 MHz, $CDCl_3$, δ): 9.61 (d, 1H, $^3J_{H-Pt}$ = 38 Hz ppy H^1, $^3J_{H1-H2}$ = 4.8 Hz), 8.85 (d, 2H, $^3J_{H-Pt}$ = 42 Hz pyrzMO H^9, $^3J_{H9-H10}$ = 5.3 Hz), 8.09 (d, 2H, pyrzMO H^{10}, $^3J_{H10-H9}$ = 5.3 Hz), 7.83 (t, 1H, ppy H^3, $^3J_{H3-H2}$ = $^3J_{H3-H4}$ = 7.7 Hz), 7.66 (d, 1H, ppy H^4, $^3J_{H4-H3}$ = 7.7 Hz), 7.49 (d, 1H, ppy H^5, $^3J_{H5-H6}$ = 7.8 Hz), 7.17 (m, 1H, ppy H^2 $^3J_{H2-H3}$ = 7.7 Hz, $^3J_{H2-H1}$ = 4.8 Hz), 7.15 (m, 1H, ppy H^6, $^3J_{H6-H7}$ = 7.5 Hz, $^3J_{H6-H5}$ = 7.8 Hz), 7.06 (t, 1H, ppy H^7, $^3J_{H7-H6}$ = $^3J_{H7-H8}$ = 7.5 Hz), 6.54 ppm (d, 1H, $^3J_{H-Pt}$ = 42 Hz ppy H^8, $^3J_{H8-H7}$ = 7.5 Hz). ^{13}C NMR (400 MHz, $CDCl_3$, δ): 163.4, 151.6, 150.4, 144.9, 139.4, 136.7, 130.5, 130.3, 129.7, 124.3, 124.1, 122.3, 118.5 ppm. ^{195}Pt NMR (400 MHz, $CDCl_3$, δ): −3243 ppm. IR-ATR (1700–1100 cm^{-1}): 1608 (s), 1581(s), 1562 (w), 1483 (s), 1458 (s), 1440 (s), 1423 (m), 1325 (s), 1304 (m), 1276 (w), 1262 (w), 1237 (w), 1218 (w), 1190 (s), 1158 (m), 1152 (w),

 This journal is © the Partner Organisations 2025

Published on 30 Mee 2025. Downloaded on 30.05.26 06:27:56.

1120 (w), 1108 (w). X-ray quality crystals were grown by slow diffusion of pentane vapour in a chloroform solution.

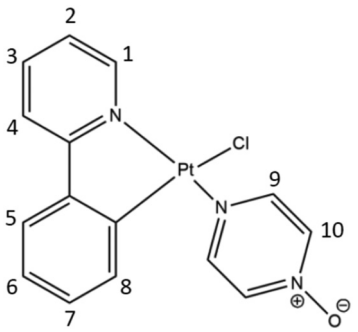

Synthesis of [Eu$_2$(tta)$_6$(μ-pyrzMOPtClppy)$_2$] (6). A solution of [PtClppy(pyrzMO)] (71.3 mg, 0.15 mmol) in 25 ml of dichloromethane was treated with [Eu(tta)$_3$] 125.7 mg (0.17 mmol). The initial bright yellow solution turned into a reddish solution. After concentrating to half volume, the product was precipitated by the addition of 50 ml of heptane. The red solid (**6**) was filtered and dried *in vacuo*. Yield: 60.4% (117.5 mg). Anal. calcd for [Eu$_2$(tta)$_6$(μ-pyrzMOPtClppy)$_2$], $C_{78}H_{48}N_6Cl_2Eu_2F_{18}O_{14}Pt_2S_6$, %: C, 36.1; H, 1.9; N, 3.2. Found: C, 35.9; H, 1.8; N, 3.0. IR-ATR (1700–1100 cm^{-1}, Fig. S3†): 1613 (w), 1597 (s), 1580 (m), 1538 (m), 1506 (w), 1487 (w), 1469 (w), 1442 (w), 1409 (m), 1353 (w), 1304 (s), 1249 (m), 1230 (m), 1188 (s), 1134 (s). X-ray quality crystals were grown by slow diffusion of pentane vapour in a dichloromethane solution.

The Gd^{3+} derivative **[Gd$_2$(tta)$_6$(μ-pyrzMOPtCl(ppy))$_2$]** (7) has been obtained following a similar procedure starting from [Gd(tta)$_3$] (128 mg, 0.177 mmol) and [PtClppy(pyrzMO)] (74.7 mg, 0,155 mmol). **7**: 142 mg, 70.4%. Anal. calcd for [Gd$_2$(tta)$_6$(μ-pyrzMOPtClppy)$_2$], $C_{78}H_{48}N_6Cl_2F_{18}Gd_2O_{14}Pt_2S_6$, %: C, 36.0; H, 1.9; N, 3.2. Found: C, 35.7; H, 1.9; N, 3.4. IR-ATR (1700–1100 cm^{-1}, Fig. S3†): 1613 (w), 1600 (s), 1580 (m), 1539 (m), 1506 (w), 1487 (w), 1456 (m), 1442 (w), 1410 (m), 1353 (w), 1305 (s), 1248 (m), 1230 (m), 1188 (s), 1137 (s). Crystals were grown by slow diffusion of pentane vapour in a dichloromethane solution. Although unsuitable for an X-ray study meeting publication standard, the crystals exhibited the same metric of **6**. Unit cell parameters have been reported in Table S2.†

Single crystal X-ray diffraction

Data was collected using an Oxford Diffraction Gemini E diffractometer, equipped with a 2K × 2K EOS CCD area detector and sealed–tube enhance (Mo) and (Cu) X-ray sources. Suitable single crystals were fastened on a nylon loop and measured at room or low temperature. Empirical multi-scan absorption corrections using equivalent reflections have been performed with the scaling algorithm SCALE3 ABSPACK. Data reduction, finalization and cell refinement were carried out through the CrysAlisPro software. Accurate unit cell parameters were obtained by least squares refinement of the angular settings of strongest reflections, chosen from the whole experiment.

The structures were solved with Olex2[99] by using ShelXT[100] structure solution program by Intrinsic Phasing and refined with the ShelXL[101] refinement package using least-squares minimization. In the last cycles of refinement, non-hydrogen atoms were refined anisotropically. Hydrogen atoms were included in calculated positions, and a riding model was used for their refinement. Refinement details for compounds **1**, **2**, **3**, **5** and **6** are given in the ESI,† together crystallographic table (Table S1†) and asymmetric unit images for all the compounds studied.

Cambridge Crystallographic Data Centre (CCDC) numbers 2395042–2395045 and 2395089† contain the supplementary crystallographic data for this paper.

Conclusions

This paper investigates dinuclear molecular lanthanide compounds with rigidly oriented pendant functional groups as building blocks for constructing d/f molecular compounds with predictable architectures. This versatile and appealing strategy highlights their role as metallo-ligands. In this study, tetranuclear Ln_2Pt_2 arrays incorporating various platinum fragments were successfully prepared using a predictable design and a flexible synthetic approach. This method enables the assembly of diverse building blocks to construct heterometallic complexes of greater complexity and facilitates the incorporation of chemical functionalization to achieve targeted functional architectures.

Concerning absorption and emission properties of Eu_2Pt_2 complexes, a straightforward visual inspection of the powdered samples reveals two distinct groups distinguishable by their colour. Compounds **1** and **3** appear as bright yellow powders, while compound **6** exhibits a darker orange hue. Notably, the absorption spectrum of **6** extends up to 600 nm, resulting in partial overlap with the most intense emission bands of Eu^{3+}. Ligand-centred energy levels proximate to the Eu^{3+} excited states favour non-radiative deactivation pathways, which can be exploited to enhance thermometric properties near room temperature. At room temperature, the emission spectra of **1** and **3** display the characteristic, well-resolved multiplets of europium. Conversely, the emission spectrum of **6** exhibits broadened signals arising from transitions between the $^5D_0$ excited state and the fundamental multiplets ^7F_J (J = 0, 1, 2, 3, and 4) of Eu^{3+}, superimposed on a background emission ascribed to Pt-containing fragment. The striking similarity in ligands between **1** and **3** accounts for their identical photoluminescence quantum yield values and luminance, approximately 10 cd m^{-2} under 375 nm LED irradiation (2.4 mW), indicating comparable light absorption capabilities. In contrast, **6** exhibits a significantly lower luminance of 0.3 cd m^{-2}.

Regarding thermometric properties, the $\Delta(T)$ curves of **1** and **3** display highly similar trends, as expected given their structural similarity. The Δ value gradually decreases with increasing temperature, following a pseudo-sigmoidal pattern. The relative thermal sensitivity (S_r) reaches a value of 1 at

Published on 30 Mee 2025. Downloaded on 30.05.26 06:27:56.

200 K and increases to 6 K^{-1}% at 300 K. For compound **6**, a steeper decrease in Δ is observed, and the temperature range in which $S_r > 1$ (T > 100 K) is approximately 100 K broader than that of compounds **1** and **3**. Previous studies on analogous compounds featuring β-diketonato units interconnected by pyrazine *N*-oxide and 4,4′-bipyridine *N*-oxide, with non-coordinated nitrogen atoms, revealed significantly higher temperatures (250–300 K) for $S_r > 1$.

The photophysical properties of Eu_2Pt_2 complexes are strongly governed by the nature of the Pt-based moieties. While PPh_3 and $AsPh_3$ ligands lead to nearly identical absorption and emission features due to their similar electronic properties, cyclometalated –PtCl(ppy) complexes exhibit significantly lower energy MLCT transitions. These states influence the thermal response of the Eu^{3+}-centred emission, with complex **6** (ppy) showing a steeper emission quenching at lower temperatures compared to complexes **1** and **3** (PPh_3, $AsPh_3$), thereby enhancing thermometric sensitivity. These findings highlight the key role of Pt-centred MLCT transitions in modulating the temperature sensitivity of Eu_2Pt_2-based luminescent thermometers and emphasize the importance of heterometallic architecture design in tailoring performance across different temperature ranges.

Data availability

All the relevant research data is included within the manuscript and ESI.†

CCDC 2395042–2395045 and 2395089† contain the supplementary crystallographic data for this paper.

Conflicts of interest

There are no conflicts to declare.

Acknowledgements

G. B. and L. A. thank the National Research Council PROGETTI@CNR P@CNR_01_ TerMoSmart, CNR projects FOE2020 - Capitale naturale e risorse per il futuro dell'Italia, FOE2022 – FuturRaw and University of Padova P-DiSC#01-BIRD2021 for financial support. L. L. and S. S. acknowledge the financial support of Pisa University (Fondi di Ateneo 2024).

References

1 N. Iki, Designing strategies for supramolecular luminescent complex of lanthanide–heterometal assembly, *Supramol. Chem.*, 2011, **23**, 160–168, DOI: **10.1080/10610278.2010.514915**.

2 M. D. Ward, Transition-metal sensitised near-infrared luminescence from lanthanides in d–f heteronuclear arrays, *Coord. Chem. Rev.*, 2007, **251**, 1663–1677, DOI: **10.1016/j.ccr.2006.10.005**.

3 M. D. Ward, Mechanisms of sensitization of lanthanide (III)-based luminescence in transition metal/lanthanide and anthracene/lanthanide dyads, *Coord. Chem. Rev.*, 2010, **254**, 2634–2642, DOI: **10.1016/j.ccr.2009.12.001**.

4 S. Faulkner, L. S. W. Natrajan, S. Perry and D. Sykes, Sensitised luminescence in lanthanide containing arrays and d–f hybrids, *Dalton Trans.*, 2009, 3890–3899, DOI: **10.1039/b902006c**.

5 K. Xu, X. Xie and L.-M. Zheng, Iridium-lanthanide complexes: Structures, properties and applications, *Coord. Chem. Rev.*, 2022, **456**, 214367, DOI: **10.1016/j.ccr.2021.214367**.

6 W. Piotrowski, K. Kniec and L. Marciniak, Enhancement of the Ln^{3+} ratiometric nanothermometers by sensitization with transition metal ions, *J. Alloys Compd.*, 2021, **870**, 159386, DOI: **10.1016/j.jallcom.2021.159386**.

7 F.-F. Chen, Z.-Q. Chen, Z.-Q. Bian and C.-H. Huang, Sensitized luminescence from lanthanides in d–f bimetallic complexes, *Coord. Chem. Rev.*, 2010, **254**, 991–1010, DOI: **10.1016/j.ccr.2009.12.028**.

8 J.-X. Liu, S.-L. Mei, X.-H. Chen and C.-J. Yao, Recent Advances of Near-Infrared (NIR) Emissive Metal Complexes Bridged by Ligands with N- and/or O-Donor Sites, *Crystals*, 2021, **11**, 155, DOI: **10.3390/cryst11020155**.

9 X. Zhu, W.-K. Wong, W.-Y. Wong and X. Yang, Design and Synthesis of Near-Infrared Emissive Lanthanide Complexes Based on Macrocyclic Ligands, *Eur. J. Inorg. Chem.*, 2011, 4651–4674, DOI: **10.1002/ejic.201100481**.

10 F.-F. Chen, H.-B. Wei, Z.-Q. Bian, Z.-W. Liu, E. Ma, Z.-N. Chen and C.-H. Huang, Sensitized Near-Infrared Emission from IrIII-LnIII (Ln = Nd, Yb, Er) Bimetallic Complexes with a (N^O)(N^O) Bridging Ligand, *Organometallics*, 2014, **33**, 3275–3282, DOI: **10.1021/om401110k**.

11 D. Li, F.-F. Chen, Z.-Q. Bian, Z.-W. Liu, Y.-L. Zhao and C.-H. Huang, Sensitized near-infrared emission of YbIII from an IrIII–YbIII bimetallic complex, *Polyhedron*, 2009, **28**, 897–902, DOI: **10.1016/j.poly.2008.12.043**.

12 K.-J. Chen, H.-B. Xu, L.-Y. Zhang and Z.-N. Chen, Cyclometalated platinum(II) complex with C^N^N tridentate ligand as sensitizer for lanthanide luminescence, *Inorg. Chem. Commun.*, 2009, **12**, 744–746, DOI: **10.1016/j.inoche.2009.06.004**.

13 R. Ziessel, S. Diring, P. Kadjane, L. Charbonniere, P. Retailleau and C. Philouze, Highly Efficient Blue Photoexcitation of Europium in a Bimetallic Pt–Eu Complex, *Chem. – Asian J.*, 2007, **2**, 975–982, DOI: **10.1002/asia.200700143**.

14 X.-L. Li, F.-R. Dai, L.-Y. Zhang, Y.-M. Zhu, Q. Peng and Z.-N. Chen, Sensitization of Lanthanide Luminescence in Heterotrinuclear $PtLn_2$ (Ln = Eu, Nd, Yb) Complexes with Terpyridyl-Functionalized Alkynyl by Energy Transfer from a Platinum(II) Alkynyl Chromophore, *Organometallics*, 2007, **26**, 4483–4490, DOI: **10.1021/om070130h**.

 This journal is © the Partner Organisations 2025

Published on 30 Mee 2025. Downloaded on 30.05.26 06:27:56.

15 F.-F. Chen, Z.-Q. Bian, Z.-W. Liu, D.-B. Nie, Z.-Q. Chen and C.-H. Huang, Highly Efficient Sensitized Red Emission from Europium(III) in Ir-Eu Bimetallic Complexes by 3MLCT Energy Transfer, *Inorg. Chem.*, 2008, **47**, 2507–2513, DOI: **10.1021/ic701817n**.

16 A. Jana, B. J. Crowston, J. R. Shewring, L. K. McKenzie, H. E. Bryant, S. W. Botchway, A. D. Ward, A. J. Amoroso, E. Baggaley and M. D. Ward, Heteronuclear Ir(III)–Ln(III) Luminescent Complexes: Small-Molecule Probes for Dual Modal Imaging and Oxygen Sensing, *Inorg. Chem.*, 2016, **55**, 5623–5633, DOI: **10.1021/acs.inorgchem.6b00702**.

17 P. Coppo, M. Duati, V. N. Kozhevnikov, J. W. Hofstraat and L. De Cola, White-Light Emission from an Assembly Comprising Luminescent Iridium and Europium Complexes, *Angew. Chem., Int. Ed.*, 2005, **44**, 1806–1810, DOI: **10.1002/anie.200461953**.

18 I. J. Al-Busaidi, R. Ilmi, J. D. L. Dutra, W. F. Oliveira, A. Haque, N. K. Al Rasbi, F. Marken, P. R. Raithby and M. S. Khan, Utilization of a Pt(II) di-yne chromophore incorporating a 2,2′-bipyridine-5,5′-diyl spacer as a chelate to synthesize a green and red emitting d–f–d heterotrinuclear complex, *Dalton Trans.*, 2021, **50**, 1465–1477, DOI: **10.1039/d0dt04198j**.

19 D. Sykes, A. J. Cankut, N. M. Ali, A. Stephenson, S. J. P. Spall, S. C. Parker, J. A. Weinstein and M. D. Ward, Sensitisation of Eu(III)- and Tb(III)-based luminescence by Ir(III) units in Ir/lanthanide dyads: evidence for parallel energy-transfer and electron-transfer based mechanisms, *Dalton Trans.*, 2014, **43**, 6414–6428, DOI: **10.1039/c4dt00292j**.

20 I. M. Etchells, M. C. Pfrunder, J. A. G. Williams and E. G. Moore, Quantification of energy transfer in bimetallic Pt(II)–Ln(III) complexes featuring an N^C^N-cyclometallating ligand, *Dalton Trans.*, 2019, **48**, 2142–2149, DOI: **10.1039/C8DT04640A**.

21 N. M. Shavaleev, L. P. Moorcraft, S. J. A. Pope, Z. R. Bell, S. Faulkner and M. D. Ward, *Chem. – Eur. J.*, 2003, **9**, 5283–5291, DOI: **10.1002/chem.200305132**.

22 N. M. Shavaleev, Z. R. Bell and M. D. Ward, *J. Chem. Soc., Dalton Trans.*, 2002, 3925–3927, DOI: **10.1039/B207832E**.

23 E. Di Piazza, L. Norel, K. Costuas, A. Bourdolle, O. Maury and S. Rigaut, d–f Heterobimetallic Association between Ytterbium and Ruthenium Carbon-Rich Complexes: Redox Commutation of Near-IR Luminescence, *J. Am. Chem. Soc.*, 2011, **133**, 6174–6176, DOI: **10.1021/ja2023515**.

24 E. Baggaley, D.-K. Cao, D. Sykes, S. W. Botchway, J. A. Weinstein and M. D. Ward, Combined Two-Photon Excitation and d/f Energy Transfer in a Water-Soluble IrIII/EuIII Dyad: Two Luminescence Components from One Molecule for Cellular Imaging, *Chem. – Eur. J.*, 2014, **20**, 8898–8903, DOI: **10.1002/chem.201403618**.

25 L.-Y. Zhang, Y.-J. Hou, M. Pan, L. Chen, Y.-X. Zhu, S.-Y. Yin, G. Shao and C.-Y. Su, Near-infrared (NIR) emitting Nd/Yb(iii) complexes sensitized by MLCT states of Ru(ii)/Ir(iii) metalloligands in the visible light region, *Dalton Trans.*, 2015, **44**, 15212–15219, DOI: **10.1039/C5DT00545K**.

26 B. J. Crowston, J. D. Shipp, D. Chekulaev, L. K. McKenzie, C. Jones, J. A. Weinstein, A. J. H. Meijer, H. E. Bryant, L. Natrajan, A. Woodward and M. D. Ward, Heteronuclear d–d and d–f Ru(ii)/M complexes [M = Gd(iii), Yb(iii), Nd(iii), Zn(ii) or Mn(ii)] of ligands combining phenanthroline and aminocarboxylate binding sites: combined relaxivity, cell imaging and photophysical studies, *Dalton Trans.*, 2019, **48**, 6132–6152, DOI: **10.1039/C9DT00954J**.

27 R. Ilmi, A. Haque, I. J. Al-Busaidi, N. K. Al Rasbi and M. S. Khan, Synthesis and photophysical properties of hetero trinuclear complexes of tris β-diketonate Europium with organoplatinum chromophore, *Dyes Pigm.*, 2019, **162**, 59–66, DOI: **10.1016/j.dyepig.2018.10.01**.

28 H.-B. Xu, L.-Y. Zhang, X.-M. Chen, X.-L. Li and Z.-N. Chen, Modulation of Pt f Ln Energy Transfer in $PtLn_2$ (Ln = Nd, Er, Yb) Complexes with 2,2′-Bipyridyl/2,2′:6′2″-Terpyridyl Ethynyl Ligands, *Cryst. Growth Des.*, 2009, **9**, 569–576, DOI: **10.1021/cg800866r**.

29 D. Rajah, M. C. Pfrunder, B. S. K. Chong, A. R. Ireland, I. M. Etchells and E. G. Moore, Sensitised lanthanide luminescence using a RuII polypyridyl functionalised dipicolinic acid chelate, *Dalton Trans.*, 2021, **50**, 7400–7408, DOI: **10.1039/D1DT00982F**.

30 C. Grechi, S. Carlotto, M. Guelfi, S. Samaritani, L. Armelao and L. Labella, Sandwich d/f Heterometallic Complexes $[(Ln(hfac)_3)_2M(acac)_3]$ (Ln = La, Pr, Sm, Dy and M = Co; Ln = La and M = Ru), *Molecules*, 2024, **29**, 3927, DOI: **10.3390/molecules29163927**.

31 S. I. Klink, H. Keizer and F. C. J. M. Van Veggel, Transition Metal Complexes as Photosensitizers for Near-Infrared Lanthanide Luminescence, *Angew. Chem., Int. Ed.*, 2000, **39**, 4319–4321, DOI: **10.1002/1521-3757(20001201)112:23<4489::AID-ANGE4489>3.0.CO;2-T**.

32 S. Faulkner and S. J. A. Pope, Lanthanide-Sensitized Lanthanide Luminescence: Terbium-Sensitized Ytterbium Luminescence in a Trinuclear Complex, *J. Am. Chem. Soc.*, 2003, **125**, 10526–10527, DOI: **10.1021/ja035634v**.

33 M. P. Placidi, A. J. L. Villaraza, L. S. Natrajan, D. Sykes, A. M. Kenwright and S. Faulkner, Synthesis and Spectroscopic Studies on Azo-Dye Derivatives of Polymetallic Lanthanide Complexes: Using Diazotization to Link Metal Complexes Together, *J. Am. Chem. Soc.*, 2009, **131**, 9916–9917, DOI: **10.1021/ja904362f**.

34 X.-F. Huang, J.-X. Ma and W.-S. Liu, Lanthanide Metalloligand Strategy toward d–f Heterometallic Metal–Organic Frameworks: Magnetism and Symmetric-Dependent Luminescent Properties, *Inorg. Chem.*, 2014, **53**, 5922–5930, DOI: **10.1021/ic403080n**.

35 A. M. Nonat, C. Allain, S. Faulkner and T. Gunnlaugsson, Mixed d-f3 Coordination Complexes Possessing Improved Near-Infrared (NIR) Lanthanide Luminescent Properties in Aqueous Solution, *Inorg. Chem.*, 2010, **49**, 8449–8456, DOI: **10.1021/ic1010852**.

Published on 30 Mee 2025. Downloaded on 30.05.26 06:27:56.

36 M. Tropiano, C. J. Record, E. Morris, H. S. Rai, C. Allain and S. Faulkner, Synthesis and Spectroscopic Study of d–f Hybrid Lanthanide Complexes Derived from triazolylDO3A, *Organometallics*, 2012, **31**, 5673–5676, DOI: **10.1021/om3003569**.

37 M. Bazi, E. Bracciotti, L. Fioravanti, F. Marchetti, M. Rancan, S. Samaritani, L. Armelao and L. Labella, Mononuclear Rare-Earth Metalloligands Exploiting a Divergent Ligand, *Inorg. Chem.*, 2024, **63**, 7678–7691, DOI: **10.1021/acs.inorgchem.3c04532**.

38 T. K. Ronson, T. Lazarides, H. Adams, S. J. Pope, D. Sykes, S. Faulkner, S. J. Coles, M. B. Hursthouse, W. Clegg, R. W. Harrington and M. D. Ward, Luminescent PtII (bipyridyl)(diacetylide) Chromophores with Pendant Binding Sites as Energy Donors for Sensitised Near-Infrared Emission from Lanthanides: Structures and Photophysics of PtII/LnIII Assemblies, *Chem. – Eur. J.*, 2006, **12**, 9299–9313, DOI: **10.1002/chem.200600698**.

39 X. L. Li, L. X. Shi, L. Y. Zhang, H. M. Wen and Z. N. Chen, Syntheses, Structures, and Sensitized Lanthanide Luminescence by Pt → Ln (Ln = Eu, Nd, Yb) Energy Transfer for Heteronuclear $PtLn_2$ and Pt_2Ln_4 Complexes with a Terpyridyl-Functionalized Alkynyl Ligand, *Inorg. Chem.*, 2007, **46**, 10892–10900, DOI: **10.1021/ic7015676**.

40 H. B. Xu, L. Y. Zhang, Z. L. Xie, E. Ma and Z. N. Chen, Heterododecanuclear Pt_6Ln_6 (Ln = Nd, Yb) arrays of 4-ethynyl-2,2′-bipyridine with sensitized near-IR lanthanide luminescence by Pt Ln energy transfer, *Chem. Commun.*, 2007, 2744–2746, DOI: **10.1039/b703135a**.

41 Q.-Y. Zhu, L.-P. Zhou and Q.-F. Sun, Strongly luminescent 5d/4f heterometal-organic macrocycles with open metal sites: post-assembly modification and sensing, *Dalton Trans.*, 2019, **48**, 4479–4483, DOI: **10.1039/C9DT00710E**.

42 H.-B. Xu, L.-Y. Zhang, Z.-H. Chen, L.-X. Shi and Z.-N. Chen, Sensitization of lanthanide luminescence by two different Pt → Ln energy transfer pathways in PtLn3 heterotetranuclear complexes with 5-ethynyl-2,2-bipyridine, *Dalton Trans.*, 2008, 4664–4670, DOI: **10.1039/b801573b**.

43 J. Li, J. Y. Wang and Z. N. Chen, Sensitized Eu III luminescence through energy transfer from PtM_2 (M = Ag or Au) alkynyl chromophores in PtM_2Eu_2 heteropentanuclear complexes, *J. Mater. Chem. C*, 2013, **1**, 3661–3668, DOI: **10.1039/C3TC30474D**.

44 A. Chandra, K. Singh, S. Singh, S. Sivakumarb and A. K. Patra, A luminescent europium(III)–platinum(II) heterometallic complex as a theranostic agent: a proof-of-concept study, *Dalton Trans.*, 2016, **45**, 494–497, DOI: **10.1039/c5dt04470g**.

45 L. Ma, L. Li and G. Zhu, Platinum-containing heterometallic complexes in cancer therapy: advances and perspectives, *Inorg. Chem. Front.*, 2022, **9**, 2424–2453, DOI: **10.1039/D2QI00205A**.

46 T. Xian, Q. Meng, F. Gao, M. Hu and X. Wang, Functionalization of luminescent lanthanide complexes for biomedical applications, *Coord. Chem. Rev.*, 2023, **474**, 214866, DOI: **10.1016/j.ccr.2022.214866**.

47 V. Fernández-Moreira and M. C. Gimeno, Heterobimetallic Complexes for Theranostic Applications, *Chem. – Eur. J.*, 2018, **24**, 3345–3353, DOI: **10.1002/chem.201705335**.

48 K. Singh, S. Singh, P. Srivastava, S. Sivakumar and A. K. Patra, Lanthanoplatins: emissive Eu(III) and Tb(III) complexes staining nucleoli targeted through Pt–DNA crosslinking, *Chem. Commun.*, 2017, **53**, 6144–6147, DOI: **10.1039/C7CC02047C**.

49 C. Alexander, Z. Guo, P. B. Glover, S. Faulkner and Z. Pikramenou, Luminescent Lanthanides in Biorelated Applications: From Molecules to Nanoparticles and Diagnostic Probes to Therapeutics, *Chem. Rev.*, 2025, **125**, 2269–2370, DOI: **10.1021/acs.chemrev.4c00615**.

50 L. Armelao, D. B. Dell'Amico, L. Bellucci, G. Bottaro, S. Ciattini, L. Labella, G. Manfroni, F. Marchetti, C. A. Mattei and S. Samaritani, Homodinuclear Lanthanide Complexes with the Divergent Heterotopic 4,4′-Bipyridine N-Oxide (bipyMO) Ligand, *Eur. J. Inorg. Chem.*, 2018, 4421–4428, DOI: **10.1002/ejic.201800747**.

51 L. Bellucci, G. Bottaro, L. Labella, V. Causin, F. Marchetti, S. Samaritani, D. B. Dell'Amico and L. Armelao, Composition–thermometric Properties Correlations in Homodinuclear Eu^{3+} Luminescent Complexes, *Inorg. Chem.*, 2020, **59**, 18156–18167, DOI: **10.1021/acs.inorgchem.0c02611**.

52 Q.-Y. Zhu, L.-P. Zhou, L.-X. Cai, S.-J. Hu, X.-Z. Li and Q.-F. Sun, Stereocontrolled Self-Assembly of Ln(III)–Pt(II) Heterometallic Cages with Temperature-Dependent Luminescence, *Inorg. Chem.*, 2022, **61**, 16814–16821, DOI: **10.1021/acs.inorgchem.2c02718**.

53 D. B. Dell'Amico, L. Labella, F. Marchetti and S. Samaritani, A convenient route to dinuclear chloro-bridged platinum(II) derivatives via nitrile complexes, *Dalton Trans.*, 2012, 1389–1396, DOI: **10.1039/C1DT11709B**.

54 D. B. Dell'Amico, L. Bellucci, L. Labella, F. Marchetti and S. Samaritani, Reactivity of platinum(II) triphenylphosphino complexes with nitrogen donor divergent ligands, *Polyhedron*, 2016, **119**, 403–411, DOI: **10.1016/j.poly.2016.09.016**.

55 D. B. Dell'Amico, S. Ciattini, L. Fioravanti, L. Labella, F. Marchetti, C. A. Mattei and S. Samaritani, The heterotopic divergent ligand N-oxide-4,4′-bipyridine (bipyMO) as directing-agent in the synthesis of oligo- or polynuclear heterometallic complexes, *Polyhedron*, 2018, **139**, 107–115, DOI: **10.1016/j.poly.2017.10.009**.

56 M. Hyeraci, L. Agnarelli, L. Labella, F. Marchetti, M. Di Paolo, S. Samaritani and L. Dalla Via, trans-Dichloro(triphenylarsino)(N,N-dialkylamino)platinum(II) Complexes: In Search of New Scaffolds to Circumvent Cisplatin Resistance, *Molecules*, 2022, **27**, 644, DOI: **10.3390/molecules27030644**.

 This journal is © the Partner Organisations 2025

Published on 30 Mee 2025. Downloaded on 30.05.26 06:27:56.

57 A. Farasat, L. Labella, F. Marchetti and S. Samaritani, Addition of Aliphatic, Secondary Amines to Coordinated Isonitriles. N-Acyclic Carbene (NAC) Platinum(II) Complexes from Trans-[Pt(μ-Cl)Cl(PPh_3)]$_2$, *Inorg. Chim. Acta*, 2022, **540**, 121062, DOI: 10.1016/j.ica.2022.121062.

58 D. B. Dell'Amico, M. Colalillo, L. Labella, F. Marchetti and S. Samaritani, Synthesis and Reactivity of Platinum(II) Triphenylphosphino Complexes with Aromatic Aldoximes, *Inorg. Chim. Acta*, 2018, **470**, 181–186, DOI: 10.1016/j.ica.2017.04.058.

59 D. B. Dell'Amico, M. Colalillo, L. Dalla Via, M. Dell'Acqua, A. N. García-Argáez, M. Hyeraci, L. Labella, F. Marchetti and S. Samaritani, Synthesis and Reactivity of Cytotoxic Platinum(II) Complexes of Bidentate Oximes: A Step towards the Functionalization of Bioactive Complexes, *Eur. J. Inorg. Chem.*, 2018, 1589–1594, DOI: 10.1002/ejic.201800055.

60 L. Dalla Via, A. N. García-Argáez, E. Agostinelli, D. B. Dell'Amico, L. Labella and S. Samaritani, New Trans Dichloro (Triphenylphosphine)Platinum(II) Complexes Containing N-(Butyl),N-(Arylmethyl)Amino Ligands: Synthesis, Cytotoxicity and Mechanism of Action, *Biorg. Med. Chem.*, 2016, **24**, 2929–2937, DOI: 10.1016/j.bmc.2016.04.067.

61 M. Hyeraci, M. Colalillo, L. Labella, F. Marchetti, S. Samaritani, V. Scalcon, M. P. Rigobello and L. Dalla Via, Platinum(II) Complexes Bearing Triphenylphosphine and Chelating Oximes: Antiproliferative Effect and Biological Profile in Resistant Cells, *ChemMedChem*, 2020, **15**, 1464–1472, DOI: 10.1002/cmdc.202000165.

62 M. Hyeraci, V. Scalcon, A. Folda, L. Labella, F. Marchetti, S. Samaritani, M. P. Rigobello and L. Dalla Via, New Platinum(II) Complexes Affecting Different Biomolecular Targets in Resistant Ovarian Carcinoma Cells, *ChemMedChem*, 2021, **16**, 1956–1966, DOI: 10.1002/cmdc.202100075.

63 D. Casanova, M. Llunell, P. Alemany and S. Alvarez, The rich stereochemistry of eight-vertex polyhedra: a continuous shape measures study, *Chem. – Eur. J.*, 2005, **11**, 1479–1494, DOI: 10.1002/chem.200400799.

64 X. Yi, G. Calvez, C. Daiguebonne, O. Guillou and K. Bernot, Rational Organization of Lanthanide-Based SMM Dimers into Three-Dimensional Networks, *Inorg. Chem.*, 2015, **54**, 5213–5219, DOI: 10.1021/acs.inorgchem.5b00087.

65 S.-L. Ma, C.-M. Qi, Q.-L. Guo and M.-X. Zhao, The novel one-dimensional chain of europium(III) complex [Eu_2(BTA)$_6$(4,4′-bpdo)]$_n$ containing dimers bridged by terminal oxygen atoms of 4,4′-bpdo molecules, *J. Mol. Struct.*, 2005, **738**, 99–104, DOI: 10.1016/j.molstruc.2004.11.031.

66 X. Yi, K. Bernot, F. Pointillart, G. Poneti, G. Calvez, C. Daiguebonne, O. Guillou and R. Sessoli, A Luminescent and Sublimable DyIII-Based Single-Molecule Magnet, *Chem. – Eur. J.*, 2012, **18**, 11379–11387, DOI: 10.1002/chem.201201167.

67 L. Fioravanti, L. Bellucci, L. Armelao, G. Bottaro, F. Marchetti, F. Pineider, G. Poneti, S. Samaritani and L. Labella, Stoichiometrically Controlled Assembly of Lanthanide Molecular Complexes of the Heteroditopic Divergent Ligand 4′-(4-Pyridyl)-2,2′:6′,2″-terpyridine N-Oxide in Hypodentate or Bridging Coordination Modes. Structural, Magnetic, and Photoluminescence Studies, *Inorg. Chem.*, 2022, **61**, 265–278, DOI: 10.1021/acs.inorgchem.1c02809.

68 L. Bellucci, L. Fioravanti, L. Armelao, G. Bottaro, F. Marchetti, F. Pineider, G. Poneti, S. Samaritani and L. Labella, Size Selectivity in Heterolanthanide Molecular Complexes with a Ditopic Ligand, *Chem. – Eur. J.*, 2023, **29**, e202202823, DOI: 10.1002/chem.202202823.

69 N. Ghavale, A. Wadawale, S. Dey and V. K. Jain, Synthesis, structures and spectroscopic properties of platinum complexes containing orthometalated 2-phenylpyridine, *J. Organomet. Chem.*, 2010, **695**, 1237–1245, DOI: 10.1016/j.jorganchem.2010.01.035.

70 M. A. Kinzhalov, S. A. Katkova, E. P. Doronina, A. S. Novikov, I. I. Eliseev, V. A. Ilichev, A. A. Kukinov, G. L. Starova and N. A. Bokach, Red photo- and electroluminescent half-lantern cyclometalated dinuclear platinum (II) complex, *Z. Kristallogr. - Cryst. Mater.*, 2018, **233**, 795–802, DOI: 10.1515/zkri-2018-2075.

71 O. Zaitceva, V. Bénétau, D. S. Ryabhukin, I. I. Eliseev, M. A. Kinzhalov, B. Louis, A. V. Vasilyev and P. Pale, *Tetrahedron*, 2020, **76**, 131029, DOI: 10.1016/j.tet.2020.131029.

72 D. S. C. Black, G. B. Deacon and G. L. Edwards, Observations on the mechanism of halogen bridge cleavage by unidentate ligands in square planar palladium and platinum complexes, *Aust. J. Chem.*, 1994, **47**, 217–227, DOI: 10.1071/CH9940217.

73 N. Godbert, T. Pugliese, I. Aiello, A. Bellusci, A. Crispini and M. Ghedini, Efficient, Ultrafast, Microwave-Assisted Syntheses of Cycloplatinated Complexes, *Eur. J. Inorg. Chem.*, 2007, 5105–5111, DOI: 10.1002/ejic.200700639.

74 A. Rodríguez-Castro, A. Fernández, M. López-Torres, D. Vázquez-García, L. Naya, J. M. Vila and J. J. Fernández, Mononuclear cycloplatinated complexes derived from 2-tolylpyridine with N-donor ligands: Reactivity and structural characterization, *Polyhedron*, 2012, **33**, 13–18, DOI: 10.1016/j.poly.2011.11.055.

75 T. Ahmed, A. Chakraborty and S. Baitalik, Terpyridyl-Imidazole Based Ligand Coordinated to Ln (Hexafluoroacetylacetonate)$_3$ Core: Synthesis, Structural Characterization, Luminescence Properties, and Thermosensing Behaviors in Solution and PMMA Film, *Inorg. Chem.*, 2024, **63**, 11279–11295, DOI: 10.1021/acs.inorgchem.4c01132.

76 A. Kourtellaris, W. Lafargue-Dit-Hauret, F. Massuyeau, C. Latouche, A. J. Tasiopoulos and H. Serier-Brault, Tuning of Thermometric Performances of Mixed Eu–Tb Metal–Organic Frameworks through Single–Crystal Coordinating Solvent Exchange Reactions, *Adv.*

Published on 30 Mee 2025. Downloaded on 30.05.26 06:27:56.

Opt. Mater., 2022, **10**, 2200484, DOI: 10.1002/adom.202200484.

77 L. K. Komodiki, N. Panagiotou, H. Serier-Brault and A. J. Tasiopoulos, Linker installation transformations in a 2-D rare earth MOF: increase of the dimensionality and turn on of the temperature sensing capability, *J. Mater. Chem. C*, 2024, **12**, 8684–8696, DOI: 10.1039/d4tc00992d.

78 H. Amouri, Luminescent Complexes of Platinum, Iridium, and Coinage Metals Containing *N*-Heterocyclic Carbene Ligands: Design, Structural Diversity, and Photophysical Properties, *Chem. Rev.*, 2023, **123**, 230–270, DOI: 10.1021/acs.chemrev.2c00206.

79 A. Galstyan, A. R. Naziruddin, C. Cebrián, A. Iordache, C. G. Daniliuc, L. De Cola and C. A. Strassert, Correlating the Structural and Photophysical Features of Pincer Luminophores and Monodentate Ancillary Ligands in PtII Phosphors, *Eur. J. Inorg. Chem.*, 2015, 5822–5831, DOI: 10.1002/ejic.201500949.

80 S. C. Gangadharappa, I. Maisuls, D. A. Schwab, J. Kösters, N. L. Doltsinis and C. A. Strassert, Compensation of Hybridization Defects in Phosphorescent Complexes with Pnictogen-Based Ligands—A Structural, Photophysical, and Theoretical Case-Study with Predictive Character, *J. Am. Chem. Soc.*, 2020, **142**(51), 21353–21367, DOI: 10.1021/jacs.0c09467.

81 R. Jordan, I. Maisuls, S. S. Nair, B. Dietzek-Ivanšić, C. A. Strassert and A. Klein, Enhanced luminescence properties through heavy ancillary ligands in [Pt(C^N^C)(L)] complexes, L = $AsPh_3$ and $SbPh_3$, *Dalton Trans.*, 2023, **52**, 18220–18232, DOI: 10.1039/D3DT03225F.

82 S. Garbe, M. Krause, A. Klimpel, I. Neundorf, P. Lippmann, I. Ott, D. Brünink, C. A. Strassert, N. L. Doltsinis and A. Klein, Cyclometalated Pt Complexes of CNC Pincer Ligands: Luminescence and Cytotoxic Evaluation, *Organometallics*, 2020, **39**, 746–756, DOI: 10.1021/acs.organomet.0c00015.

83 R. Jordan, S. Kler, I. Maisuls, N. Klosterhalfen, B. Dietzek-Ivanšić, C. A. Strassert and A. Klein, Synthesis and Photophysics of the Doubly Cyclometalated Pd(II) Complexes [Pd(C^N^C)(L)], L = PPh_3, $AsPh_3$, and $SbPh_3$, *Inorg. Chem.*, 2025, **64**, 6561–6574, DOI: 10.1021/acs.inorgchem.4c05436.

84 L. Bellucci, L. Babetto, G. Bottaro, S. Carlotto, L. Labella, E. Gallo, F. Marchetti, S. Samaritani and L. Armelao, Competing excitation paths in Luminescent Heterobimetallic Ln-Al complexes: unravelling interactions via experimental and theoretical investigations, *iScience*, 2023, **26**, 106614, DOI: 10.1016/j.isci.2023.106614.

85 S. Carlotto, L. Babetto, L. Bellucci, G. Bottaro, F. Marchetti, S. Samaritani, L. Labella and L. Armelao, Understanding Stabilization Factors in Heterodinuclear Ln-Al Complexes from DFT Simulations on Thermochemistry Data: A Counterintuitive Conclusion, *Inorg. Chem.*, 2024, **63**, 16702–16712, DOI: 10.1021/acs.inorgchem.4c02021.

86 K. Yanagisawa, Y. Kitagawa, T. Nakanishi, T. Seki, K. Fushimi, H. Ito and Y. Hasegawa, A Luminescent Dinuclear EuIII/TbIII Complex with LMCT Band as a Single-Molecular Thermosensor, *Chem. – Eur. J.*, 2018, **24**, 1956–1961, DOI: 10.1002/chem.201705021.

87 K. Yanagisawa, Y. Kitagawa, T. Nakanishi, T. Akama, M. Kobayashi, T. Seki, K. Fushimi, H. Ito, T. Taketsugu and Y. Hasegawa, Enhanced Luminescence of Asymmetrical Seven-Coordinate EuIII Complexes Including LMCT Perturbation, *Eur. J. Inorg. Chem.*, 2017, 3843–3848, DOI: 10.1002/ejic.201700815.

88 P. P. Ferreira da Rosa, S. Miyazaki, H. Sakamoto, Y. Kitagawa, K. Miyata, T. Akama, M. Kobayashi, K. Fushimi, K. Onda, T. Taketsugu and Y. Hasegawa, Coordination Geometrical Effect on Ligand-to-Metal Charge Transfer-Dependent Energy Transfer Processes of Luminescent Eu(III) Complexes, *J. Phys. Chem. A*, 2021, **125**, 209–217, DOI: 10.1021/acs.jpca.0c09337.

89 Y. Kitagawa, P. P. Ferreira da Rosa and Y. Hasegawa, Charge-transfer excited states of π- and 4f-orbitals for development of luminescent Eu(III) complexes, *Dalton Trans.*, 2021, **50**, 14978–14984, DOI: 10.1039/D1DT03019A.

90 V. I. Tsaryuk, K. P. Zhuravlev and P. Gawryszewska, Processes of luminescence quenching in europium aromatic carboxylates with the participation of LMCT states: A brief review, *Coord. Chem. Rev.*, 2023, **489**, 215206, DOI: 10.1016/j.ccr.2023.215206.

91 W. Thor, H.-Y. Kai, Y. Zhang, K.-L. Wong and P. A. Tanner, Thermally Activated Photophysical Processes of Organolanthanide Complexes in Solution, *J. Phys. Chem. Lett.*, 2022, **13**, 4800–4806, DOI: 10.1021/acs.jpclett.2c01350.

92 A. Carlotto, L. Babetto, S. Carlotto, M. Miozzi, R. Seraglia, M. Casarin, G. Bottaro, M. Rancan and L. Armelao, Luminescent Thermometers: From a Library of Europium (III) β-Diketonates to a General Model for Predicting the Thermometric Behaviour of Europium-Based Coordination Systems, *ChemPhotoChem*, 2020, **4**, 674–684, DOI: 10.1002/cptc.202000116.

93 C. Blais, G. Calvez, Y. Suffren, C. Daiguebonne, C. Paranthoen, E. Bazin, S. Freslon, K. Bernot and O. Guillou, Luminance and Brightness: Application to Lanthanide-Based Coordination Polymers, *Inorg. Chem.*, 2022, **61**, 19588–19596, DOI: 10.1021/acs.inorgchem.2c03500.

94 K. L. Wong, J. C. G. Bünzli and P. A. Tanner, Quantum yield and brightness, *J. Lumin.*, 2020, **224**, 117256, DOI: 10.1016/j.jlumin.2020.117256.

95 K. Binnemans, Interpretation of Eu(III) Spectra, *Coord. Chem. Rev.*, 2015, **295**, 1–45, DOI: 10.1016/j.ccr.2015.02.015.

96 W. Lu, B. X. Mi, M. C. W. Chan, Z. Hui, C. M. Che, N. Zhu and S. T. Lee, Light-Emitting Tridentate Cyclometalated Platinum(II) Complexes Containing ó-Alkynyl Auxiliaries: Tuning of Photo- and Electrophosphorescence, *J. Am. Chem. Soc.*, 2004, **126**, 4958–4971, DOI: 10.1021/ja0317776.

 This journal is © the Partner Organisations 2025

97 C. F. Koelsch and W. H. Gumprecht, Some Diazine-N-Oxides, *J. Org. Chem.*, 1958, **23**, 1603–1606.
98 L. Armelao, D. B. Dell'Amico, L. Bellucci, G. Bottaro, L. Labella, F. Marchetti and S. Samaritani, A Convenient Synthesis of Highly Luminescent Lanthanide 1D-Zigzag Coordination Chains Based Only on 4,4′-Bipyridine as Connector, *Polyhedron*, 2016, **119**, 371–376, DOI: **10.1016/j.poly.2016.09.009**.
99 O. V. Dolomanov, L. J. Bourhis, R. J. Gildea, J. A. K. Howard and H. Puschmann, OLEX2: A complete structure solution, refinement and analysis program, *J. Appl. Crystallogr.*, 2009, **42**, 339–341, DOI: **10.1107/S0021889808042726**.
100 G. M. Sheldrick, SHELXT - Integrated space-group and crystal-structure determination, *Acta Crystallogr., Sect. A: Found. Crystallogr.*, 2015, **71**, 3–8, DOI: **10.1107/S2053273314026370**.
101 G. M. Sheldrick, Crystal structure refinement with SHELXL, *Acta Crystallogr., Sect. C:Cryst. Struct. Commun.*, 2015, **71**, 3–8, DOI: **10.1107/S2053229614024218**.

Published on 30 Mee 2025. Downloaded on 30.05.26 06:27:56.